CONSTRAINTS ON THE GENESIS OF COBALT DEPOSITS: PART II, APPLICATIONS TO NATURAL SYSTEMS

O.V. Vasyukova and A.E. Williams-Jones

Department of Earth and Planetary Sciences, McGill University, 3450 University Street Montréal, Québec, Canada, H3A 0E8

Abstract

Cobalt is in high demand because of the key role that cobalt-lithium ion batteries are playing in addressing the issue of global warming, particularly in facilitating the transition from the internal combustion engine to electrically-driven vehicles. In a companion paper (Williams-Jones and Vasyukova, 2021), we review the properties of cobalt, its mineralogy and the processes that concentrate it to exploitable levels. Using this information and knowledge of the geology of the principal types of cobalt deposits, the present paper assesses the conditions and controls of cobalt transport and deposition and develops/refines plausible models for the genesis of these deposits. Economic cobalt deposits owe their origin to the compatible nature of Co^{2+}, which caused it to concentrate in the mantle, mainly in olivine, and to be released to magmas only after high degrees of partial melting (i.e., to komatiitic and basaltic magmas). There is, thus, a very close association between cobalt deposits and mafic and ultramafic rocks. Primary magmatic deposits, in which Co is subordinate to Ni, develop through sulfide-silicate liquid immiscibility as a result of the very strong preference of these metals for the sulfide liquid. Predictably, these deposits reach their highest grades where hosted by olivine-rich ultramafic rocks. Approximately 60% of the World's cobalt resource is of hydrothermal origin and is contained in sediment-hosted copper deposits in the Democratic Republic of the Congo. Using a combination of thermodynamic data and geological information, we have refined a model, in which Co is leached from mafic and ultramafic rocks by oxidized, chloride-rich hydrothermal fluids, derived from evaporation, and deposited in response to decreasing fO_2 in carbonaceous sediments that accumulated in intracratonic rift basins. Economic Co deposits also develop as hydrothermal vein systems, in which Co is the primary ore metal. In the only deposits of this type that are currently being exploited (Bou Azzer, Morocco), the source of the Co was an adjacent serpentinized ophiolite. The ore fluid was an oxidized, high salinity brine derived from evaporites and deposition occurred in response to pH neutralization by

the felsic igneous host. The final major class of Co deposits is laterite-hosted and develops on olivine-rich ultramafic rocks or their serpentinized equivalents. Our thermodynamic modeling shows that Co is leached from an ultramafic source by mildly acidic fluids as Co^{2+} and is transported down the laterite profile, eventually concentrating by a combination of adsorption on Mn oxides, incorporation in the structure of absolane, a Mn oxide, and precipitation as heterogenite, a cobalt oxy-hydroxide. The dissolution of cobalt at the surface and its deposition at depth are controlled mainly by pH, which decreases downwards; oxygen fugacity, which also decreases downwards, has the opposite effect, inhibiting dissolution of cobalt at the surface and promoting it at depth. It is our hope that this introduction to the economic geology of cobalt and the processes responsible for the formation of cobalt-bearing ores will help guide future studies of cobalt ore genesis and strategies for the exploration of this critical metal.

Introduction

An increased demand for cobalt (mostly for batteries and super-alloys required by the automotive and aerospace industries, but also by the chemical industry and in medicine) has created a strong need to find new resources of this metal. Most (>50 %) of the current cobalt supply is a by-product of the mining of copper in the Democratic Republic of the Congo (DRC) from sediment-hosted hydrothermal deposits of the Central African Copperbelt that straddles the border between the DRC and Zambia (Slack et al., 2017). The remaining cobalt comes from magmatic sulfide deposits (23 %) and laterites (15 %). In both cases, it is associated with mafic and ultramafic rocks and is a by-product of nickel mining. The only primary producers of cobalt are hydrothermal vein-type deposits in the Bou Azzer district, Morocco, which occur along the contacts between serpentinites and quartz diorite intrusions or felsic volcanic rocks (En-Naciri et al., 1997, Dolansky, 2007, Bouabdellah et al., 2016).

In a companion paper (Williams-Jones and Vasyukova, 2021), we evaluated the main processes that contribute to the concentration of cobalt to exploitable levels. These processes include the fractional crystallization of magmas, magmatic liquid immiscibility, and the mobilization of cobalt by aqueous fluids at ambient and higher temperature. We showed that, because of the highly compatible nature of cobalt, only mafic and ultramafic magmas, produced as a result of high degrees of partial melting, can acquire the cobalt concentrations needed to form magmatic ores. Cobalt, however, concentrates more readily in ultramafic magmas, typically reaching

concentrations more than twice those of mafic magmas. Further concentration is possible by fractional crystallization. Thus, in the case of basaltic magmas, fractional crystallization can produce olivine cumulates for which the Co content is similar to or even higher than that of ultramafic magmas. The main magmatic process concentrating cobalt to economic levels, however, is sulfide-silicate immiscibility. Owing to the very strong preference of Co for the sulfide liquid over the silicate liquid, with an appropriate R factor (silicate/ sulfide mass ratio) and accumulation of the sulfide liquid, the enrichment in Co of the final rock can be considerable. Hydrothermal mobilization of Co can also lead to the concentration of cobalt to exploitable levels, particularly if the ore fluid is saline and oxidized. At lower temperature, Co is predicted to deposit efficiently (as sulfide minerals) in response to a sharp reduction in fO_2, whereas at higher temperature the most likely cause of Co mineral deposition is an increase in pH. In this paper, we build on the theoretical framework established in Williams-Jones and Vasyukova (2021) and make use of the published literature to develop/refine plausible models for the genesis of the principal cobalt deposit types.

Cobalt deposits

Magmatic deposits

Magmatic Ni-Co sulfide deposits result from the separation of immiscible sulfide liquids from silicate liquids of komatiitic or basaltic composition, and the partitioning of the cobalt into the sulfide liquid. As komatiitic magmas typically have much higher concentrations of cobalt than basaltic magmas (greater than twice as high on average; Williams-Jones and Vasukova, 2021), the ore deposits produced by the separation of sulfide liquids from these magmas should have higher cobalt concentrations than those exsolved from basaltic magmas. Whether or not an economic deposit forms from either magma type will likely depend, however, on the availability of sulfur, the R or N factor and the physico-chemical conditions.

Komatiite-hosted deposits

Komatiite-associated magmatic sulfide deposits occur at or near the base of komatiite flows and range from tens of thousands of tonnes (e.g., Alexo, Canada: 115 Kt grading 700 ppm Co; Barnes and Naldrett, 1986, Houlé et al., 2012) to tens (e.g., Kambalda, Australia; 67 Mt grading 2,070 ppm Co; Naldrett, 2004b) and hundreds of millions of tonnes (e.g., Mt Keith, Australia; 478 Mt

grading 140 ppm Co; Naldrett, 2004b). The flows typically take the form of ribbon-like shoots, which, in the case of the Kambalda Camp, range up to 2,500 m in length and 300 m in width and occupy channels that are interpreted to reflect thermal erosion of the underlying volcano-sedimentary substrate (Fig. 1). Two major types of ore have been recognised, massive and matrix. The massive ores, exemplified by Kambalda, occur at the base of komatiitic flows (Fig. 2a), which are meters to tens of meters thick, and pass upwards into the matrix ores, in which the sulfides form a continuous network interstitial to cumulate olivine (Hoatson et al., 2006). In some cases, e.g., Mt Keith, the massive ores are absent and, instead, the deposits are dominated by matrix and overlying disseminated mineralization, which is commonly developed well above the base of the flows (Fig. 2b). In both types of deposits, the main ore minerals are pyrrhotite, pentlandite and chalcopyrite with subordinate magnetite and chromite. Pentlandite, which forms a solid solution with cobaltpentlandite, is the main host to cobalt.

In order for a komatiitic magma to host an economic deposit, it needs to have a high enough concentration of sulfur to form a significant mass of immiscible Fe-sulfide liquid. Although early models of the genesis of komatiite-hosted magmatic sulfide deposits assumed that the mantle was the source of the sulfur (Naldrett et al., 1979), it is now generally agreed that extruded komatiitic magmas are highly undersaturated with respect to sulfur. The reason for this is the low S content of the mantle (~200 ppm) and the fact that the sulfur saturation concentration of mafic and ultramafic magmas increases with decreasing pressure (Mavrogenes and O'Neill, 1999). The generally agreed upon source for the sulfur is the sulfidic graphitic sedimentary rocks that commonly underlie komatiite-hosted magmatic sulfide deposits (Lesher and Groves, 1986, Williams et al., 2011, Houlé et al., 2012); this association is common because of the emplacement of komatiitic magmas in rift-related euxinic basins (Lesher and Groves, 1986). Accordingly, komatiitic magmas are widely interpreted to have acquired their sulfur by thermally eroding and assimilating these sedimentary rocks, as first proposed by Huppert et al. (1984). This interpretation is supported by $\delta^{34}S$ values for the magmatic sulfides, which are very similar to those of the sedimentary sulfides (Lesher and Groves, 1986), and elevated concentrations of highly incompatible lithophile elements in the komatiites, which is consistent with a significant crustal component (Houlé et al., 2012).

Although the Co grades of komatiite-hosted magmatic sulfide deposits range up to ~2,000 ppm (Kambalda district; see above) the Co concentration in the 100% sulfide fraction is much higher, and in the case of the Kambalda district, is ~9,940 ppm (Naldrett, 2004b). In order to explain the latter concentration, we applied the model presented in Williams-Jones and Vasyukova (2021) that predicts the concentration of metals in an immiscible sulfide liquid based on the initial concentration of the metal in the silicate magma, the sulfide-silicate partition coefficient for this metal and the silicate-sulfide mass ratio (R or N). For an oxygen fugacity corresponding to that of the graphite-CO_2 buffer (chosen to reflect the assimilation of graphitic sediments), the partition coefficient for Co between a sulfide liquid and a komatiitic melt (D_{Co}) would be 83 at 1,400 °C; by comparison for a fO_2 corresponding to the FMQ buffer the value of D_{Co} would be 31 at this temperature. Using a value for D_{Co} of 83, the Co concentration of the sulfide liquid would be of the order of ~8,000 ppm, assuming a Co concentration in the komatiitic magma of 104 ppm and a R factor of 1,000. If, however, the temperature were decreased to 1,300 °C to take account of the cooling effect of thermal erosion (D_{Co} increases to 92), and the initial Co content of the komatiite magma was increased by just 15 ppm (119 ppm), the Co content of the sulfide liquid would be 10,036 ppm, i.e., comparable to that of the 100% sulfide fraction of the Kambalda ore. Finally, we raise the possibility that some of the sedimentary sulfide did not dissolve in the komatiite magma but formed excess liquid globules that interacted with the magma, further concentrating the cobalt. In summary, komatiite-associated magmatic Co deposits owe their existence to the common occurrence of sulfidic graphitic sediments, which supplied the necessary sulfur and, by lowering the fO_2 of the system, favored a Co sulfide-silicate liquid partition coefficient high enough to concentrate Co to the levels observed in these deposits.

Gabbro-associated deposits

The gabbro-associated class of magmatic Co deposits is dominated by two groups of deposits, namely, Sudbury (Canada), which contains 2,648 Mt of ore grading 380 ppm Co and Noril'sk-Talnakh (Russia) with 1,309 Mt of ore grading 610 ppm Co (Slack et al., 2017). They are followed by the Pechenga deposits (Russia) with 339 Mt of ore grading 450 ppm Co and the Voisey's Bay deposit (Canada) with 137 Mt grading 900 ppm Co (Slack et al., 2017). It is noteworthy that these Co grades are several times lower than those of komatiite-hosted magmatic deposits. As the Sudbury deposit is unique, having formed as a result of a meteorite impact, and our objective is to

provide generalized descriptions of representative deposits applicable to any gabbro-hosted Co mineralization, the Sudbury deposit is not considered further in this paper.

The Noril'sk-Talnakh deposits are hosted by three flattened, tube-like, gabbroic sills cogenetic with the Siberian continental flood basalt event (248±2.4 Ma; Campbell et al., 1992) that helped define the Permian-Triassic boundary; there are also at least 20 sills or suites of sills that are subeconomic or barren (Naldrett, 2004c). The three ore-bearing sills range in thickness from 50 to 300 m, extend along strike for over 15 km, are hosted either by coal-bearing siliciclastic sedimentary rocks of the Permian Tungusskaya series (the Noril'sk and Talnakh intrusions) or by locally organic-rich siliciclastic sedimentary rocks of the Lower Devonian Razvedochninsky Formation (the Kharaelakh intrusion). The sills are surrounded by thick metasomatic aureoles that increase in thickness with the degree of mineralization (Iacono-Marziano et al., 2017). The sulfide mineralization forms a massive layer up to 45 m thick that occurs at the base of the sills or intrudes the underlying sedimentary rocks, and is overlain by taxitic olivine gabbro and, in turn, by picritic gabbro; both the latter units contain disseminated sulfides (Fig. 3a). For many of the metals (particularly, the chalcophile metals), the tenor increases upwards from the massive ore through the disseminated ore in taxitic gabbro to the disseminated ore in picritic gabbro (Naldrett, 2004c). Significantly, the proportions of metals in the ore bodies are much greater than normally would be expected for sills of the thickness reported above (Naldrett et al., 1996). Pyrrhotite is the dominant sulfide mineral and is accompanied by pentlandite and chalcopyrite. The bulk of the Co is hosted by pentlandite. An important feature of the sulfide mineralization is its heavy sulfur isotope signature, with $\delta^{34}S$ values that vary between ~8 and ~14 ‰; in individual deposits, the $\delta^{34}S$ values are very homogeneous (Malitch et al., 2014). These very high $\delta^{34}S$ values provide strong evidence of an external source for the sulfur (magmatic sulfur has a δ34S value of 0 ± 3; Ohmoto, 1986). The fact that they differ amongst deposits also implies that the corresponding magma batches were contaminated to different degrees. As the Devonian sedimentary sequence (dominantly carbonates) contains numerous anhydrite-bearing evaporite horizons, the obvious source for the sulfur is anhydrite, which in these rocks has a $\delta^{34}S$ value of ~20 ‰ (Gorbachev and Grinenko, 1973). Assimilation of anhydrite also would have increased fO_2 sharply, thereby promoting the solubility of sulfur; there is an order of magnitude increase in the solubility of sulfur in basaltic magmas at fO_2 values > 1-2 log units above the QFM buffer (Jugo, 2009). This, in turn, would have led to a need for a reductant at the site of ore deposition (coal measures in the case of Noril'sk

and Talnakh and organic-rich siliciclastic rocks in the case of Karaelakh) to decrease the sulfur carrying capacity of the magma and ensure exsolution of large masses of immiscible sulfide liquid. Although there is general agreement that the large size and high metal grade of the Noril'sk-Talnakh deposits was the result of assimilation of crustal (evaporitic) sulfur and the availability of a reductant, there is considerable debate over some aspects of the genesis of the deposits. Some of the issues for which there is little agreement are whether the intrusions represent the conduits for the magma forming the Siberian traps (Naldrett, 2004c), or terminated near the ore bodies (Krivolutskaya et al., 2018), whether the sulfur was assimilated by the magma on its way to the surface (Arndt et al., 2003) or in long-lived staging chambers (Malitch et al., 2014) and whether the sulfide liquid exsolved in a magma chamber (Naldrett, 2004c) or at the site of intrusion (Iacono-Marziano et al., 2017). The model that we favour is one in which a mantle plume produced basaltic magmas that ascended along normal faults (rift setting) into the upper crust, where they assimilated Devonian carbonate sedimentary rocks containing variable proportions of anhydrite, intruded higher level siliciclastic sedimentary rocks parallel to bedding, where they thermally eroded coal measures (Noril'sk and Talnakh) or organic-rich sedimentary rocks (Karaelakh), depositing a sulfide liquid, and continued to the surface to form the Siberian traps (Fig. 3b). This model calls for ore formation at the site of intrusion, for the sills being the conduits for the magma, explains the wide metasomatic aureoles that surround the intrusions as being the product of aqueous-carbonic fluids produced by coal assimilation (Iacono-Marziano et al., 2017) and, most importantly, by invoking an open system, satisfactorily addresses the issue of why the metal tenors greatly exceed those predicted by the observed mass of silicate rocks in the intrusions (Naldrett et al., 1996).

The 1.98 Ga Pechenga deposits, which are located in the Kola peninsula of Russia, provide another example of deposits associated with a continental flood basalt event, in this case, focussed on the Pechenga-Varzuga rift system (Naldrett, 2004a). The deposits are associated with syn-volcanic sill-like mafic/ultramafic intrusions, 10-600 m thick and 100-3000 m in strike length, that are concentrated in two intrusive/eruptive centers, ~ 18 km apart, namely the Kaula center in the west and the Pilgujärvi center in the east (Naldrett, 2004a). The sills intruded sulfidic black shales of the Pilgujärvi Sedimentary Formation, also known as the Productive Formation, which is underlain and overlain by flood basalts of the Kolasjoki and Pilgujärvi Volcanic Formations, respectively (Melezhik and Sturt, 1994). In contrast to the Noril'sk-Talnakh sills, the Pechenga sills

differentiated into a lower wehrlite (olivine-clinopyroxene peridotite) and an upper gabbro (Abzalov and Both, 1997, Naldrett, 2004a). As was the case for the Noril'sk-Talnakh intrusions, the sills are comagmatic with flows; the latter form the lower part of the Pilgujärvi basaltic succession, i.e., just above the Productive Formation (Melezhik and Sturt, 1994). The orebodies are located mainly in wehrlite at the base of the intrusions and have been classified into breccia ore (where the bottom of an intrusion has been tectonized), massive ore, and net-textured to disseminated ore that overlies the massive ore (Abzalov and Both, 1997). There was also some remobilization of the ores into quartz-carbonate veins during subsequent serpentinization and associated talc-carbonate alteration. Pyrrhotite comprises 50 to 80 vol.% of the primary ores and is accompanied by 5 to 25 vol.% pentlandite and chalcopyrite. Although there is no information available on the ore-mineral hosting the Co, by analogy with other gabbro-hosted deposits, it is almost certainly pentlandite. As noted above, the sills intruded into sulfidic black shales of the Productive Formation, which would have been an obvious source for the sulfur in the deposits. The $\delta^{34}S$ sulfide maxima, however, vary from ~0 ‰ in deposits in the western, Kaula, intrusive/eruptive center to ~+5 ‰ in the eastern, Pilgujärvi, center (Abzalov and Both, 1997, Naldrett, 2004a), suggesting that there was more than one source of sulfur. Abzalov and Both (1997), therefore, proposed that the ores in the western center had a juvenile source, but those in the eastern center were the products of assimilation of sulfidic shales from the Productive Formation. As discussed earlier, a juvenile sulfur source for the ores seems highly unlikely because, on emplacement in the crust, mantle-derived magmas are undersaturated with the respect to sulfide. Moreover, $\delta^{34}S$ values for diagenetic pyrite of the Productive Formation are characterized by two populations, an early diagenetic population with values between -2.7 ‰ and +2.6 ‰ and a later diagenetic population with values ranging from +0.9 ‰ to +24.9 ‰ (Melezhik et al., 1998). Therefore, Melezhik et al. (1994), as discussed in Naldrett (2004a), attributed the different sulfur isotope signatures of the ores of the western and eastern centers to assimilation of early diagenetic pyrite of an incompletely lithified Productive Formation and assimilation of late diagenetic pyrite from this formation, respectively. More recently Hanski et al. (2011) have used trace element and, particularly Re-Os isotopic data, to argue that at least some parts of the ore-forming magma were sulfide-saturated prior to their injection into the sulfide-rich Productive Formation black shales, and suggested that some of the sulfur may have come from the sulfide-rich, 50-150 m thick, Black Shale member in the middle of the underlying Kolasjoki Volcanic

Formation. Irrespective of the location of the black shales that may have interacted with the ore-forming magma, there is little doubt that the Pechenga magmatic Co deposits owe their origin to assimilation of sulfidic black shales. A model that satisfactorily explains the various features of the deposits and their hosts is the ascent of a mantle-derived ferropicritic magma along the Pechenga-Varzuga rift, its interaction with sulfidic black shales and differentiation to form wehrlite-gabbro sills, saturation of the magma with a sulfide liquid largely at the site of intrusion, possible magma renewal to add to the metal budget (and feed the overlying flows), and remobilization of the resulting Ni-Cu-Co-PGE ores as a result of ongoing rift-related deformation (Naldrett, 2004a).

The Voisey's Bay deposit is hosted by a 1.33 Ga gabbro-troctolite intrusion belonging to the Nain Plutonic Suite, which is located along the boundary between the Proterozoic Churchill Province and the Archean Nain Province (Li and Naldrett, 1999). The intrusion comprises a large troctolite body (the Eastern Deeps), which was fed from below by a feeder dyke, and several other ovoid bodies made up largely of massive sulfide. Within the Eastern Deeps, the massive sulfides are concentrated near the base of the intrusion, particularly in the vicinity of the feeder dyke. The Voisey's Bay intrusion is hosted by Proterozoic paragneiss (Tasiuyak gneiss) comprising interlayered sulfide- and graphite-bearing garnet-sillimanite and quarto-feldspatic gneisses, and Archean orthogneiss. Locally, the paragneisses contain up to 30 modal % pyrrhotite (sulfidic interlayers) and 10 modal % graphite (graphitic interlayers). These gneissses, therefore, are the probable source for the external sulfur required to ensure saturation of the magma with a sulfide liquid. Support for this interpretation is provided by the facts that variably assimilated xenoliths of Tasiuyak gneiss are observed in the intrusion, that the $\delta^{34}S$ values of the ores range from 0 ‰ down to -4.1 ‰ and that the $\delta^{34}S$ values of the Tasiuyak gneissses vary between -0.9 and -17 ‰ (Ripley et al., 1999). The model favored for the genesis of the Voisey's Bay deposit is the interaction of a mantle-derived picritic magma with the Tasiuyak gneisses to produce a gabbroic troctolite magma that acquired a significant proportion of its sulfur by assimilating sulfide-(graphite)-rich layers in the gneisses and consequently saturated with a sulfide liquid into which the metals (Ni, Cu, Co and PGE) partitioned preferentially (Ripley et al., 1999, Naldrett, 2004d).

In the preceding paragraphs, we have shown that the formation of gabbro-associated magmatic sulfide deposits depends on the availability of an external source of sulfur. For the Noril'sk-

Talnakh deposits, the source was anhydrite from evaporites and for the Pechenga deposits, black shale-hosted sulfide minerals. In the case of the Voisey's Bay deposits, the source for sulfur was a pelitic (garnet-sillimanite) paragneiss, which, given the high proportion of both sulfide and graphite, likely represents a precursor black shale. Whether the source of the sulfur is sulfidic sediments or evaporites will have a strong impact on the degree of super-saturation. As discussed by Williams-Jones and Vasyukova (2021) and mentioned above, assimilation of evaporites is accompanied by a potentially large increase in the fO_2 of the magma and consequently, the solubility of sulfur. Subsequent reduction of fO_2, such as was the case for the Noril'sk-Talnakh deposits, could, therefore, lead to a very high degree of super-saturation. In contrast, assimilation of sulfidic sediments (organic rich) would lead to a much lower degree of super-saturation that would be independent of fO_2. Thus, we predict that the silicate/sulfide ratio was low for Noril'sk-Talnakh and high for Pechenga and Voisey's Bay. In principle, this ratio (R for a closed system and N for an open system) can be estimated from the initial concentration of Co in the silicate magma, the Co concentration of the 100 % sulfide ore and the sulfide-silicate Co partition coefficient (for further discussion, see Williams-Jones and Vasyukova, 2021). In the case of the Noril'sk-Talnakh deposits, we assumed the initial Co concentration in the magma to have been 44 ppm, which corresponds to the average Co content of Siberian flood basalts in the vicinity of Noril'sk (Lightfoot et al., 1993), that the value of D_{Co} was 68 (see Williams-Jones and Vasyukova, 2021) and that the Co content of the 100% sulfide Noril'sk-Talnakh ore was 1078 ppm (based on the Ni/Co ratio and Ni content reported in Naldrett, 2004c). As the system is considered to have been open (see above), the corresponding silicate/sulfide mass ratio is predicted to have been ~30. In contrast, for Pechenga, the silicate/sulfide mass ratio would have been >10,000 assuming a value of D_{Co} of 43 (calculated using the equation of Li and Audétat, 2015, from the FeO content of an average ferropicrite chill margin in the district of 15.05 wt.%, Hanski and Smolkin, 1995, for a temperature of 1200 °C, a pressure of 500 bar and fO_2 buffered by graphite-CO_2), an initial Co concentration in the magma of 86 ppm (Hanski and Smolkin, 1995) and a Co content of the 100% sulfide ore of 4034 ppm (Naldrett, 2004a). These calculations confirm that the degree of sulfide super-saturation at Noril'sk-Talnakh was orders of magnitude higher than at Pechenga. Unfortunately, it was not possible to determine an R or N factor for Voisey's Bay because of the absence of information on the magma that produced the deposit.

In summary, gabbro-associated magmatic deposits have considerably lower Co concentrations than komatiite-hosted deposits but, like the latter, depend on a major contribution from an external sulfur source. The much lower Co grades of the gabbro-, gabbro-wehrlite- and gabbro-troctolite-hosted deposits relative to the komatiite-hosted deposits likely reflect the much lower concentration of Co in the magma and/or lower value of D_{Co}. More generally, Co grades for both gabbro- and komatiite-associated magmatic deposits are strongly affected by the silicate-sulfide mass ratio and in some cases by oxygen fugacity (sulfur solubility and sulfide-silicate partition coefficients for Co are strongly fO_2 dependant).

Hydrothermal deposits

Sediment-hosted cobalt deposits

As has already been noted, the bulk of the World's cobalt is produced by the Democratic Republic of the Congo. The cobalt occurs in the "Copperbelt", which comprises a suite of Proterozoic silici-clastic and carbonate sedimentary rocks (≤880 to ≥735 Ma; Key et al., 2001, Master et al., 2005) that have been metamorphosed to greenschist facies and locally to higher grade. Although cobalt is present in both the Congolese and Zambian parts of this belt, the cobalt/copper ratio is much higher in the Congo (1:13 vs 1:57 on average, and locally reaches 3:1; Cailteux et al., 2005).

The rocks hosting the "Copperbelt" deposits formed in sub-basins of a large Neoproterozoic intracratonic rift basin and are part of a succession of continental, marginal marine and sub-wave metasedimentary rocks referred to collectively as the Roan Group (Cailteux et al., 2005). Two phases of rifting have been recognized, the first of which is represented by the dominantly siliciclastic rocks (sandstones and conglomerates) of the Lower Roan Group. This phase of rifting reached a climax in the Congo with the precipitation of evaporites (Bull et al., 2011), and was followed by a marine transgression during which siltstones, dolomitic siltstones and then shales of the Mines Subgroup were deposited (Cailteux et al., 2005, Selley et al., 2018). The succeeding sedimentation (Dipeta Subgroup) accompanied a marine regression and involved deposition of argillaceous sandstones, shallow marine carbonates and eventually evaporites. This marked the end of sedimentation associated with the first phase of rifting. The second phase coincided with an abrupt change to deeper water conditions (another marine transgression) and the deposition of reduced siltstones and shales of the Mwashya Subgroup (the uppermost member of the Roan

Group) that was accompanied by mafic magmatism represented by interbedded volcanic rocks and gabbroic sills (Selley et al., 2018).

Virtually all the Cu-Co mineralization is hosted by reduced (organic-rich) argillaceous sedimentary rocks of the lower Mines Subgroup and, to a much lesser extent, the Mwashya Subgroup (Cailteux et al., 2005, Selley et al., 2018). The bulk of it is also stratiform and occurs either in layers or in nodules that are interpreted by Cailteux et al. (2005) to have replaced anhydrite and gypsum. Based on evidence of differential compaction around the nodules, this soft sediment deformation, is interpreted to indicate that the mineralization was emplaced before lithification and thus to be either syngenetic or diagenetic in origin (Cailteux et al., 2005). A diagenetic origin, however, is preferred because of the association of the ores with authigenic quartz (Dewaele et al., 2006).

The main cobalt ore mineral is carrollite (Table 1), but in some deposits, there is abundant cattierite and/or linnaeite and/or siegenite; cobaltpentlandite and cobaltite have been observed in some deposits (Cailteux et al., 2005). These minerals occupy pore space among detrital grains and are accompanied by Cu sulfides (chalcopyrite, bornite and chalcocite), pyrite, authigenic quartz, chlorite and dolomite (Cailteux et al., 2005, Dewaele et al., 2006). The earliest ore minerals to deposit were Cu-bearing framboidal pyrite and slightly later Co-Ni-bearing pyrite. Cattierite deposited contemporaneously with the Co-Ni-bearing pyrite (Cailteux et al., 2005). This was followed by deposition of chalcopyrite, followed by bornite + carrolite and, finally, chalcocite (El Desouky et al., 2010). Linnaeite deposited contemporaneously with carrollite. The cobalt minerals are irregularly distributed but, in the Mines Subgroup, generally reach their highest concentrations in the upper, copper-poor parts of the orebodies, indicating that the two metals are zonally distributed (Cailteux et al., 2005). In the orebodies hosted by the Mwashya Subgroup, Co is a minor component and there is no obvious zonation in the distribution of carrollite and the other Co minerals. A similar separation of Co and Cu to that in the Mines Subgroup has been reported for the equivalent unit in Zambia, the Copperbelt Orebody Member (also referred to as the Ore Shale), although in the Copperbelt Orebody member, Co may be enriched relative to Cu in either the footwall or the hangingwall of the Cu orebodies (Annels and Simmonds, 1984). In addition, some deposits in the underlying arenites are characterized by a lateral zonation of Cu and Co, in which chalcopyrite and bornite (and some carrollite) occur proximal to the basin margin, and Co minerals

are distributed distally from it, in the sequence (with increasing distance), carrollite, linnaeite and cobaltpentlandite (Annels and Simmonds, 1984).

The deposits were subjected to deformation and metamorphism during the Lufilian Orogeny at ~560–550 Ma (Porada and Berhorst, 2000), during which vein- and breccia-hosted mineralization developed (El Desouky et al., 2009, 2010), including economic deposits that are associated with sodic alteration (Selley et al., 2018). There is, however, little agreement on the source of the Co and Cu for these deposits, i.e., whether these metals were remobilized from the stratiform orebodies and/or introduced later (Hitzman et al., 2005, Dewaele et al., 2006). Finally, it is noteworthy that many of the deposits underwent supergene enrichment during the Cretaceous and Tertiary (Hitzman et al., 2005).

A major issue for the genesis of the stratiform deposits is the source of the metals. Although some authors have suggested that red beds in the lower part of the Roan Group (R.A.T. Sub-group) may have been the source (Haynes, 1986), most authors have advocated a source in the underlying metamorphic basement (e.g., Cailteux et al., 2005, Hitzman et al., 2005). The focus, however, has been the source of the Cu, and the issue of a source for Co has not been addressed explicitly. Moreover, no explanation has been put forward for why the deposits in the Congolese part of the Copperbelt are much more enriched in Co than they are in Zambia. As discussed earlier, Co concentrations are relatively low in most rock types, and only attain significant concentrations in mafic (~40 ppm) and particularly in ultramafic igneous rocks (> 100 ppm). It, therefore, seems very likely that the Co was sourced by mafic-ultramafic rocks. Significantly, mafic-ultramafic complexes of Kibaran age (1.0-1.3 Ga) containing up to 160 ppm Co (the ultramafic units contain 134 ppm Co on average; Duchesne et al., 2004) occur in a belt (the Kabanga-Musongati Line) that extends from Burundi to Angola (Kunene Intrusive Complex; Ernst et al., 2013) beneath the northernmost part of the “Copperbelt”. Even more significantly, the most Co-rich deposits of the DRC occur in this area, e.g., the Musonoi deposit, which contains ~185 Kt of Co and has a Cu:Co ratio of ~4:1 (Taylor et al., 2013). We, therefore, propose that mafic-ultramafic complexes in the basement were the source of the cobalt in the northernmost Co-rich part of the DRC and, possibly, for Co-rich deposits elsewhere in the “Copperbelt”.

Despite a general agreement that the Cu-Co mineralization was diagenetic in origin and formed in a rift setting, the nature of the fluid, its origin and the conditions of mineralization are poorly constrained. In large part, this is because the rocks hosting the early mineralization were subjected to deformation and greenschist facies metamorphism during the Lufilian orogeny. Several studies have reported fluid inclusion data for the "Copperbelt" (Greyling, 2009, and references therein, Davey, 2019), but to our knowledge only Dewaele et al. (2006) have reported data for primary inclusions that can be reliably interpreted to represent the mineralizing fluid for the stratiform ores. These inclusions, which occur in authigenic quartz intergrown with carrollite, bornite and chalcocite, have an average salinity of ~15 wt.% NaCl eq. and homogenize at an average temperature of ~160 ^{o}C. Given the unconsolidated nature of the sediments and consequent shallow burial depth, this temperature also likely represents the temperature of mineralization.

Additional insight into the nature and origin of the fluids and the mineralizing process is provided by sulfur isotopic data and halogen chemistry. The S-isotopic data show that the ores are characterized by a wide range in $\delta^{34}S$ values (-10.3 to +3.1; El Desouky et al., 2010), which would be consistent with either bacterial sulfur reduction (BSR) or thermochemical sulfate reduction (TSR) of a sulfate-rich fluid of evaporitic origin, i.e., the residue of evaporation or dissolution of evaporite. Based on the Cl, Br and Na contents of leachates of ore only and ore and gangue mixtures, these fluids are interpreted to be residues of the evaporation of seawater (Selley, et al., 2018).

Although a large number of studies has been devoted to the deposits of the "Copperbelt", quantitative evaluation of the genesis of the Co mineralization has remained elusive. This is mainly because of a lack of information on the stability of the Co ore minerals that has prevented determination of the physicochemical conditions of mineralization. Here, we make use of the results of our earlier analysis of the behavior of cobalt in aqueous solutions and Co sulfide phase equilibria (Williams-Jones and Vasyukova, 2021) to evaluate the physicochemical conditions of Co ore formation in the "Copperbelt". Unfortunately, we were unable to consider carrollite (the main Co mineral) because of a lack of thermodynamic data for this phase. However, as carrollite is isostructural with linnaeite, it is reasonable to surmise that predictions made for the behavior of linnaeite may be applicable to carrollite.

In evaluating the physicochemical controls on mineralization, we assumed that the ore fluid had a salinity of 15 wt.% NaCl, that Co was transported as a chloride complex ($CoCl_4^{2-}$) and the temperature was 150 °C (see above). The sulfur concentration was estimated to be 0.003 m, assuming that this fluid was saturated with anhydrite; the $CaCl_2$ concentration was assumed to be 3.75 wt.%, which represents 25% of the total salinity, the maximum permitted by the eutectic data reported by Dewaele et al. (2006), and is within the range reported by Greyling (2009) for fluid inclusions interpreted to have been trapped immediately after mineralization. The initial pH of the fluid is estimated to have been ~ 5.5, based on our modeling of the aqueous speciation using the HCh software package (Shvarov and Bastrakov, 1999). Oxygen fugacity would have been in the sulfate predominance field and, in order to transport significant Co, would have been ≥ -43, i.e., approximately four log units above the hematite-magnetite (HM) buffer (Fig. 4; constructed using the program GeoTPD, Bastrakov and Dick, 2019).

A rough estimate of the fO_2 during Co mineral deposition can be made from the common occurrence of reduced carbon in the ore horizons and the presence of both CO_2- and CH_4-bearing fluid inclusions in the ores (e.g., Greyling, 2009). Assuming equal proportions of CO_2 and CH_4, the corresponding value of $\log fO_2$ would have been ~-48, or ~1 log unit below the HM buffer. Although the pH during ore deposition may have changed as a result of fluid-rock interaction, the overall change is likely to have been small. This is because the oxidation of carbonaceous material to CO_2 would have decreased pH by forming carbonic acid, whereas hydration of silicate minerals and dissolution of calcite would have had the opposite effect. It is, therefore, reasonable to assume that the pH did not change significantly from its initial value of 5.5. At the above fO_2 and this pH (red circle in Fig. 4), all of the dissolved Co would have precipitated, and done so largely as cattierite, a relatively common Co-sulfide in the ores. Thus, the estimated decrease in fO_2 alone would have been sufficient to explain the formation of the deposits. In order to explain the observed mineral paragenesis (cattierite→linnaeite→cobaltpentlandite), however, it is necessary to invoke an additional parameter. A decrease in the sulfur activity with fluid evolution, for example, as a result of fluid-rock interaction (sulfidation of the Fe in silicate minerals), could produce this paragenesis. This decrease would lead to a shrinkage in the size of the cattierite stability field that could be sufficient to allow for continued precipitation of Co in the stability field of linnaeite. In contrast, although a decrease in temperature would have further induced Co mineral deposition, it would have expanded the field of stability of cattierite, thereby, inhibiting deposition

of linnaeite and cobaltpentlandite (Williams-Jones and Vasyukova, 2021). In summary, the modeling described above and the available geological evidence suggest strongly that a decrease in fO_2 was the main cause of Co ore-formation.

An interesting and potentially important feature of the Co mineralization mentioned earlier is that it is zoned vertically and horizontally (Zambian Copperbelt) in respect to the Cu mineralization. Moreover, where horizontally zoned, the Cu mineralization is close to the edge of the basin, whereas the Co mineralization is distal to it and, with increasing distance into the basin, occurs in the sequence carrolite, linnaeite and cobaltpentlandite (Annels and Simmonds, 1984). This suggests that Cu was less soluble than Co. In order to test this hypothesis, we evaluated the solubility of Cu in the fluid described above for the same conditions as those employed for Co. For simplicity, and to provide a direct comparison to Co, we only considered minerals in the Cu-O-S system and, thus, ignored chalcopyrite and bornite, which would have required introducing Fe into the system. Based on the results of our modelling, it is evident, just as it was for Co, that for a pH range including the value of 5.5 considered above, Cu transport is promoted by high fO_2 and Cu mineral solubility (represented by chalcocite, a common Cu mineral in the ores) decreases sharply with decreasing fO_2 (Fig. 4). Most significantly, at the same conditions of fO_2 and pH, the solubility of chalcocite is orders of magnitude lower than that of the cobalt minerals. This explains the zonation of Cu and Co minerals described above and supports our earlier conclusion that decreasing fO_2 was the principal driver of Co ore-deposition.

Using the information presented above, we propose the following model for the formation of stratiform Co ores of the type found in the DRC. This model involves the production of oxidized sulfate-bearing saline ore fluids from the evaporation of seawater (Selley et al., 2018), a process culminating with the formation of evaporite horizons during the accumulation of clastic and carbonate sediments in an intracratonic rift basin. The resulting fluids, therefore, had the high oxygen fugacity and salinity necessary for them to efficiently transport Co (and Cu). According to the model (Fig. 5), these fluids were heated by rift-related magmatic activity and expelled repeatedly from the sedimentary pile into the adjacent basement rocks during marine transgressions, as a result of the increased pressure within the sediments and seismic activity associated with ongoing rifting. After interaction with Kibaran mafic and ultramafic rocks in the basement that enriched them in Cu and Co, respectively, these heated, pregnant, saline brines were

"pumped" back seismically (Sibson et al., 1975) into the sedimentary package during marine regressions (due to the decreased pressure within the sediments) and infiltrated the unconsolidated organic-rich sediments (Fig. 5). There, they precipitated Co and Cu sulfide minerals in response to the sharp decrease in fO_2 and increased activity of H_2S that accompanied reduction of the fluid (including sulfate) by organic matter. Owing to the much lower solubility of the Cu minerals relative to the Co minerals with decreasing fO_2, this led to orebodies that are characterized by proximal (to the basement) and distal assemblages of Cu and Co minerals, respectively. In summary, the cobalt-rich ores of the "Copperbelt" formed as a result of: 1) the availability of saline, oxidized evaporitic residual fluids; 2) access of these fluids to Co-Cu enriched mafic-ultramafic basement rocks; 3) fluid "pumping" induced by the pressure changes accompanying transgression/regression (rising/falling sea level) and seismicity; and 4) the presence of organic-matter in the host rocks, which caused the sharp decrease in fO_2 required for mineralization.

Vein-hosted cobalt deposits

Vein-hosted cobalt deposits, also referred to as "five-element vein-type deposits" because many of them are also enriched in Ni, As, Ag, and Bi (Halls and Stumpfl, 1972), comprise deposits consisting dominantly of Co-Ni-Fe arsenides that have been mined for cobalt and/or silver, notably the deposits of the Erzgebirge (Germany), the Great Bear Lake and Cobalt-Gowganda districts (Canada) and the Bou Azzer district (Morocco). Of these deposits, only those of the Bou Azzer district are currently in production and they are responsible for ~2 % of the World's cobalt supply (Slack et al., 2017). The mineralization of vein-hosted cobalt deposits can also be stratabound and/or of replacement type. They also occur in a variety of rock-types and geological settings (Scharrer et al., 2019). There is, however, a very consistent paragenesis characterized by early deposition of native elements, a second stage of arsenide (typically in the sequence Ni→Co→Fe) and sulfarsenide deposition, and a late sulfide stage, comprising base metal sulfides and Ag-, Sb- and As-bearing sulfosalts (Scharrer et al., 2019). Here, we describe the deposits of the Bou Azzer district to represent this five element or vein-hosted class of arsenide deposits and propose a model, which explains their formation that may be applicable to other deposits of this type.

More than 60 orebodies have been exploited in the Bou Azzer mining district, all of which are located along the borders of serpentinite massifs from a Neoproterozoic (697±8 Ma;El Hadi et al., 2010) ophiolite fragment that was intruded by diorite and quartz-diorite prior to and during its

emplacement. This fragment is overlain by dacitic to rhyolitic ignimbrites and andesitic tuffs, intercalated with red beds of the Ouarzazate formation (~575 Ma; Mifdal and Peucat, 1985) and, in turn, by peritidal carbonates, red beds and evaporites (gypsum-bearing) of the Adoudou formation (~540 Ma; Gasquet et al., 2005, Maloof et al., 2005). The Co deposits are much younger, as shown by age estimates based on U, Th and Pb concentrations in brannerite (366 Ma ± 9 Ma; Dolansky, 2007) and radiometric ages of 310 ± 5 Ma and 308 ± 31 Ma reported by Oberthür et al. (2009) for brannerite (U-Pb) and calcite (Sm-Nd), respectively; both brannerite and calcite were coeval with the Co mineralization. The latter ages are close to K-Ar ages (330-320 Ma) of the Intra Visean stage of the Hercynian orogeny, which is known to have affected this part of Morocco (Hoepffner et al., 2005).

The orebodies take the form of subvertical veins and lenses located at the contact between the serpentinites and quartz-diorites/diorites, as well as subhorizontal tabular masses that are sandwiched between the tops of the serpentinites and the overlying volcanic succession. Adjacent to the ore bodies, the serpentinite was altered to talc and the quartz-diorite/diorite or volcanics to chlorite; these host rocks were also silicified. This alteration can be expressed by the following idealized reactions:

$$\text{(Lizardite) } Mg_3Si_2O_5(OH)_4 + 2H_4SiO_4^{\circ} = \text{(Talc) } Mg_3Si_4O_{10}(OH)_2 + 5H_2O \quad (1)$$

$$\text{(Magnesiohornblende) } Ca_2[Mg_4Al]Si_7AlO_{22}(OH)_2 + Mg^{2+} + 2H^{+} + 10H_2O = \text{(Clinochlore) } Mg_5Al(Si_3Al)O_{10}(OH)_8 + 2Ca^{2+} + 4H_4SiO_4^{\circ} \quad (2)$$

The ore bodies comprise lenses and veins that may extend up to 600 m along strike and reach 20 m in width, although most are much narrower (1 to 2 m wide). Crack-and-seal textures are common, and, locally, may occur on a fine scale, bearing witness to repeated episodes of vein opening and closing. There is also evidence for extensive brecciation of the host rock and cementation of the fragments by arsenides, sulfarsenides and sulfides. The main cobalt ore minerals are skutterudite, safflorite and cobaltite (Table 1), which are accompanied by variable proportions of ankerite and dolomite. In most deposits, skutterudite was the first mineral to crystallize followed by safflorite and/or cobaltite. Locally, crystallization of safflorite alternated with that of cobaltite in rhythmic sequences separated by intervals of precipitation of dolomite or ankerite (Dolansky, 2007).

Fluid inclusion studies have shown that the Co mineralization was produced by a high salinity NaCl-$CaCl_2$-rich (~40 wt.% NaCl eq.) aqueous fluid at a temperature of ~250 ºC (Dolansky, 2007). A similar conclusion about the temperature (265 ºC) was reached from the sulfur isotopic compositions of pyrite and barite (Levresse, 2001). The sulfur isotope compositions also provide insights into the fO_2 conditions and the potential source of the fluid. Indeed, the wide range of the values of $\delta^{34}S$ for chalcopyrite (9.9 to -6.8 ‰; Maacha, 1998, Dolansky, 2007) is strong evidence that the mineralizing fluid was highly oxidized (such a range is consistent with sulfide precipitation in the sulfate predominance field; Ohmoto, 1972). Furthermore, the $\delta^{34}S$ value of barite (25.7 ‰) reported by (Maacha, 1998) is consistent with an evaporitic origin for the fluid. At 250 ºC the corresponding $\delta^{34}S$ of the fluid would be +24 ‰ (calculated using the AlphaDelta online software of Beaudoin and Therrien, 2009), which is within the range of typical seawater compositions (Kampschulte and Strauss, 2004). A likely source for the sulfur is the gypsum of the evaporite-bearing 'Calcaires inférieurs' of the upper Adoudou Formation (Álvaro et al., 2008), which outcrops in the vicinity of several of the deposits of the Bou Azzer district. Based on the oxygen and hydrogen isotopic data (7.9-9.6 ‰ for $\delta^{18}O^{fluid}$ and -42.4 ‰ for δD^{fluid}) presented in Dolansky (2007), the source of the fluid could have been magmatic or metamorphic. The fluid could also have been seawater or meteoric water that equilibrated with igneous or metamorphic rocks. As there is no evidence for igneous activity of an age similar to that of the mineralization and as this age coincides with that of the Hercynian orogeny, we propose that the ore fluid was a metamorphic water or meteoric water that equilibrated with metamorphic rocks and that this water acquired its sulfur (see above) and high salinity from the evaporites of the upper Adoudou Formation ('Calcaires inférieurs').

Although several models have been proposed for the genesis of the Bou Azzer deposits, there is no consensus on their origin other than that the source of the Co is the serpentinite (for further information on previously proposed genetic models, see Bouabdellah et al., 2016). The Bou Azzer serpentinites contain ~160 ppm Co, most of which is concentrated in magnetite (3,000 ppm), and are the only rocks in the area that host significant concentrations of Co. Based on the observations presented above, we propose that the Bou Azzer deposits formed from meteoric and/or metamorphic fluids after interaction with the ~540 Ma Adoudou evaporites and that the main driver of hydrothermal activity was the high heat flow associated with the Hercynian orogeny. The high salinity and oxidation state of these fluids provided the capacity to effectively mobilize cobalt

(see the discussion of aqueous cobalt transport in Williams-Jones and Vasyukova, 2021) and deliver it to the site of ore deposition.

A major issue for any model of the genesis of the Bou Azzer deposits is the source of arsenic. Previous studies have suggested that either the serpentinites or the overlying late Neoproterozoic volcanic cover may have been this source. The only direct evidence, that one of them could have been the source, however, is for the serpentinites, which contain traces of realgar and As-bearing magnetite (Leblanc and Billaud, 1982). It is also possible that these rocks contained a lot more arsenic that was subsequently lost and/or consumed to make the deposits. Indeed, considerable arsenic can accumulate in ultramafic rocks as a result of their serpentinization by seawater, which, because it involves a very high seawater/rock ratio (1000 - 17,000; Frisby et al. 2016), makes up for the low concentration of As in seawater (1.7 ppm on average; Neff et al., 2002). Reliable determination of the concentration of As during serpentinization is not possible but, if we speculate that 10% of the As was removed from the seawater, a process that would be facilitated by the fact that As adsorbs efficiently onto the surface of brucite (Lafay et al., 2016), which forms during serpentinization, the amount of As accumulated might have been in the range 170 to 2,890 ppm. This amount is similar to or exceeds that of Co in the Bou Azzer serpentinite (160 ppm), the likely source of the metal for the deposits, suggesting that the serpentinite could easily have been the source of the arsenic for the cobalt ores. The other source that has been proposed for the arsenic is ignimbrite of the late Neoproterozoic volcanic cover. Although such rocks are reported to occur at unspecified localities in the Anti-Atlas and contain 100-300 ppm As (Leblanc and Billaud, 1982), to our knowledge, there is no record of ignimbrites proximal to Bou Azzer.

A source for the arsenic that has not been considered previously is the upper Adoudou Formation, which we proposed above was the source of the sulfur and salinity of the ore fluid. Although evaporites normally do not have elevated concentrations of arsenic, there are some important exceptions to this, e.g., the Miocene evaporites of the Anatolian plateau (Turkey) and the Puna high plateau of Argentina (Helvaci and Alonso, 2000). Arsenic in these evaporites occurs as orpiment and realgar (commonly in association with gypsum; Helvaci and Alonso, 2000) and, in some cases, e.g., the Emet deposit (Turkey), its concentration may exceed a thousand ppm (Erdoğan et al., 1998). The key feature, in the context of the current study, which distinguishes these As-bearing evaporites, is that their formation was coeval with volcanism, as shown by the

intercalation of the evaporites with tuffs of felsic to intermediate composition and evidence of hot spring activity; in the Emet deposit, the tuffs may contain > 1,000 ppm As. This association of evaporite with volcanic activity is also a feature of the 'Calcaires inférieurs' of the Adoudou Formation, which contains litharenites of pyroclastic origin intercalated with the anhydrite-bearing carbonate rocks and is capped by an acidic tuff, both potentially sourced by the Alougoum volcanic complex (the associated Boho volcano is located < 10 km south of Bou Azzer; Álvaro et al., 2006, 2008). Although the presence of arsenic has not been reported for the Adoudou Formation, it is noteworthy that arsenic, as the $[AsO_3]^{2-}$ ion, substitutes for the sulfate ion and potentially can be immobilized as gypsum or anhydrite (Lin et al., 2013). In principle, the same is true for calcite or dolomite through the substitution of $[AsO_3]^{2-}$ for $[CO_3]^{2-}$ (Di Benedetto et al., 2006). For the reasons given above, it is therefore plausible that the evaporites of the 'Calcaires inférieurs' of the Adoudou Formation were the source, not only of the sulfate-bearing brines involved in cobalt transport, but also the arsenic required for ore formation.

Based on the preceding discussion, we propose a two-stage model in which hot, high salinity, oxidized S-bearing hydrothermal fluids reacted with serpentinite, leached Co by oxidizing magnetite to hematite, transported it as the chloride species $CoCl_4^{2-}$ and deposited it as arsenides and sulfarsenides in the adjacent quartz-diorites, diorites and volcanics. The first stage (Fig. 6a) involved the release of Co (Ni, Fe, Cu) to the fluid followed by the immediate precipitation these metals as sulfides due to the reduction of the fluid because of the oxidation of magnetite to hematite; sulfide-rich zones containing linnaeite, Co pentlandite, chalcopyrite, bornite and millerite have been reported to occur in the serpentinite (Leblanc and Billaus, 1982). Any As present in the fluid or in the serpentinite would have precipitated as realgar (Guillemette and Williams-Jones, 1993), traces of which were also reported by Leblanc and Billaus (1982) in the sulfide-rich zones. This initial stage occurred at a low fluid-rock ratio (approaching unity), which ensured a high concentration of Co in the fluid. The second stage (Fig. 6b) involved remobilization of Co, which commenced when the fO_2 buffering capacity of the serpentinite decreased due to the consumption of magnetite, and the fluid became progressively more oxidized. This fluid dissolved the earlier formed sulfides and re-deposited the metals as arsenides and sulfarsenides along the contact between the serpentinites and the host rocks (quartz-diorite, diorite or volcanics), where fractures opened in response to differences in the competence of the two rock suites and the fluid-rock ratio was consequently high.

A distinguishing feature of the "five-element vein-type" deposits, including those at Bou Azzer, is that the Co mineralization takes the form of arsenides and sulfarsenides rather than sulfides, as, for example, was the case for the sediment-hosted deposits of the "Copper Belt". We attribute the arsenic-rich nature of the Bou Azzer ores to a combination of a high As concentration and the highly oxidized nature of the fluid, which resulted in a low reduced:oxidized sulfur ratio, thereby placing the fluid in the predominance field of sulfate or bi-sulfate and inhibiting saturation with Co sulfides.

Deposition of skutterudite, the earliest of the cobalt ore minerals at Bou Azzer, is interpreted to have occurred as a result of the reaction:

$$CoCl_4^{2-} + 3H_3AsO_3^0 = CoAs_3 + 4Cl^- + 2H^+ + 3.5H_2O + 2.75O_2 \quad (3)$$

In principle, this deposition could have been caused either by an increase in pH or a decrease in fO_2. A decrease in fO_2, however, can be ruled out because it would have caused reduction of the sulfate (or bi-sulfate) and, therefore, precipitation of the cobalt in the form of sulfide, as was the case in the serpentinite (see above). The lack of a suitable reductant at the site of deposition (in the diorite/quartz-diorite and volcanics or at the contact between these units and the serpentinite) is further support for the conclusion that skutterudite deposition did not result from a reduction in fO_2. Thus, although Scharrer et al. (2019) have argued that a decrease in fO_2 is the main control on the deposition of Co arsenides without Co-sulfides (because of the kinetic difficulty of reducing sulfate to sulfide and the ease of reducing arsenite to arsenide), for the reasons given above, we propose that skutterudite deposited because of an increase in pH (Reaction 3), a hypothesis, which is consistent with the alteration observed in the host diorites/volcanics (Reaction 2).

In principle, the evolution of the paragenesis from skutterudite to an alternation of safflorite and cobaltite can be explained by either: 1) an increase in fO_2 accompanied by a decrease in pH (Fig. 5c, dashed arrow); or 2) a decrease in the As:S (reduced) ratio that displaced fO_2-pH conditions to the stability boundary of the latter two minerals (Fig. 6d). The first scenario can be excluded because the change in fO_2-pH conditions would lead to a sharp increase in solubility (Fig.6c) and, therefore, cobalt mineral dissolution rather than deposition. The second scenario, however, is a predictable consequence of the evolution of the fluid to lower As concentration resulting from the progressive depletion of As in the source due to continued fluid rock interaction. This would have

been the case, if the source of As was the serpentinite but is more difficult to envisage if the source was the evaporite (see earlier discussion of source). We, therefore, propose that the cobalt mineral paragenesis changed from skutterudite to safflorite/cobaltite because of a decrease in the As:S (reduced) ratio and that this decrease occurred because the As was sourced dominantly by the serpentinite.

In conclusion, whether they are sediment- or vein-hosted, hydrothermal Co deposits result from the interaction of highly saline, oxidized brines with ultramafic rocks and the dissolution of Co as chloride species. The source of the brines in the two examples considered was an evaporite or in the case of the "Copperbelt" the residue of evaporation, and, for the arsenide, vein-hosted class, evaporite may also have been the source of the As, although a serpentinite source seems more likely. The key to whether an arsenide or sulfide deposit forms is not only the As concentration of the fluid but also the ratio of As to reduced S. Oxygen fugacity decrease was the key factor in the deposition of the sediment-hosted Co ores, whereas pH increase was a major factor in the deposition of the vein-hosted ores.

Laterite deposits

The final class of deposits that makes a major contribution to the global cobalt resource is the laterite class. These deposits form over ultramafic rocks and their serpentinized equivalents as a result of weathering in hot, humid tropical climates and are mined primarily for Ni; even in Co-rich deposits the Ni:Co ratio is typically > 10:1 (Slack et al., 2017). They also are a potentially important source of scandium (Williams-Jones and Vasyukova, 2018). Nickel-cobalt laterites have been subdivided into three broad types to recognize the different hosts for the Ni, i.e., oxides (dominantly goethite), hydrous Mg-silicates (serpentine and talc) and clay silicates (smectites) (Brand et al., 1998). Cobalt concentrations, however, reach their highest levels in oxide-type laterites, particularly those developed over olivine-rich peridotites and komatiites (Freyssinet et al., 2005). Laterites developed over pyroxenites have distinctly lower Co concentrations. Economic deposits (>50 Mt and >1 wt.% Ni) typically have Co grades in the range 0.07 to 0.15 wt.% Co (0.1 wt.% on average) and a Ni:Co wt.% ratio of 12.7 on average (Slack et al., 2017). For comparison, the average Ni:Co ratio of peridotites is 18.

A typical oxide laterite profile varies between 25 and 50 meters in thickness and is generally subdivided from the base up into: 1) saprock, which has experienced <20 % weathering and contains > 20 wt% MgO; 2) saprolite that contains relicts of primary olivine and pyroxene (or pre-weathered serpentine); 3) yellow laterite (limonitic) that contains abundant goethite, Mn oxides and chalcedony and <2 wt.% MgO; 4) red laterite (hematitic) that is distinguished from the underlying yellow laterite by a higher content of clay minerals, and 5) ferricrete, a ferruginous horizon in which the soil particles have been cemented by iron hydroxides. Cobalt concentrations are low in the ferricrete and red laterite and reach a maximum in the lower part of the yellow laterite, below which they decrease gradually to the background value of the ultramafic precursor. The maximum concentration (~ 0.3 wt. % in Co-rich deposits; Llorca, 1993) coincides with an elevated proportion of Mn oxides, e.g., lithiophorite or cryptomelane, to which the Co was adsorbed and absolane, a cobaltiferous or nickeliferous Mn-oxide. In deposits that are particularly enriched in Co, the cobalt also occurs as heterogenite, and in these deposits there is a clear upward zonation from heterogenite through cobaltiferous absolane to cryptomelane and lithiophorite (Llorca, 1993). In contrast, Ni commonly reaches its maximum concentration lower in the profile, i.e., in the saprolite, where it occurs either in Fe and/or Mn oxides or, if the bedrock rock has been heavily serpentinized, as garnierite, a material comprising serpentine, talc, chlorite and sepiolite (Butt and Cluzel, 2013).

The key factors leading to the formation of an economic Ni-Co deposit are the nature of the bedrock, the climate and the geomorphology. Cobalt-rich laterite deposits form almost exclusively over olivine-rich ultramafic rocks and their serpentinized equivalents. Tectonically, they are found mainly (~ 85%;Freyssinet et al., 2005) in the accretionary terranes of the Circum-Pacific, the Caribbean and the Balkans, where ophiolites abound. They also occur in cratonic terranes, where the peridotite-rich parts of layered mafic igneous complexes or komatiitic volcanics are exposed. The nature of the laterite varies depending on the relief. In areas of relatively low relief, such as on cratons, the water table is high, water flow-rates are low and the intensity of leaching is low, leading to limited mobilization of the metals (Freyssinet et al., 2005). Where the relief is higher, as in accretionary terranes, the water table is deep, water flow-rates are high and leaching is intense, leading to a maximum metal enrichment in the lower parts of the profile (Golightly, 1981). It is in this environment that the Co-rich oxide laterites are best developed.

Nickel-cobalt laterite formation begins with the leaching of Mg and some Si from olivine (much of the Si precipitates as quartz or chalcedony), forming goethite as shown by the reaction:

$$(Fe,Mg)_2SiO_4 + 2\,H^+ + 0.25O_2 = SiO_2 + FeOOH + Mg^{2+} + 0.5\,H_2O$$

Olivine Quartz Goethite

This is typically followed by the hydrolysis of serpentine to form saponite and goethite via the reaction:

$$2\,(Mg,Fe)_3Si_2O_5(OH)_4 + 2.5\,H_2O + 0.75\,O_2 = Mg_3Si_4O_{10}(OH)_2.4H_2O + 3FeOOH$$

Serpentine Saponite Goethite

which is accompanied or preceded by the oxidation to goethite of any magnetite produced during the serpentinization of olivine via the reaction:

$$Fe_3O_4 + 1.5\,H_2O + O.25\,O_2 = 3\,FeOOH$$

Magnetite Goethite

These reactions release cobalt, which is dissolved in the weathering fluid for subsequent concentration by adsorption on Mn oxides like lithiophorite and cryptomelane, incorporation in the structure of absolane and precipitation as heterogenite. They also lead to the development of a ferricrete in the upper part of the profile, where hematite largely replaces goethite in the reactions.

In order to gain further insight into the process of Co concentration in Ni-Co laterites, we modelled the solubility of heterogenite in an idealised laterite profile, assuming that cobalt is mobilized as Co^{2+}, which is the dominant cobalt species at ambient temperature in chloride-free systems (see Williams-Jones and Vasyukova, 2021), except at very high pH, and that Co^{2+} precipitates as heterogenite according to the reaction:

$$Co^{2+} + 1.5\,H_2O + 0.25\,O_2 = CoOOH + 2\,H^+$$

As is evident from this reaction, the solubility of heterogenite depends on both pH and oxygen fugacity, increasing with decreasing pH and decreasing fO_2. The pH for the profile was constrained by the measurements of water extracted from a Ni-Co laterite by van der Ent et al. (2013). These measurements show that the pH at the top of a profile is ~ 5.5 (due to the interaction of meteoric water with humic acids), that it increases to 6.5 in the yellow (limonitic) laterite and to 7 in the

saprolite (water in equilibrium with unaltered ultramafic rocks has a pH of ~8). For comparison, Gleeson et al. (2004) reported a pH of 8.1 from ground water springs at the base of a Ni laterite (saprock) in Columbia. The only information that, to our knowledge, is available on oxygen fugacity in a laterite profile is that of Parc et al. (1989) for a manganese laterite and was obtained from an evaluation of phase equilibria data involving a suite of manganese oxides. Two oxides in this suite commonly occur in Ni-Co laterites, namely lithophorite and cryptomelane. We assumed that the value of log fO_2 reported by Parc et al. (1989) for lithiophorite (-10.8) corresponded to the oxygen fugacity at the top of the yellow laterite, that the value of log fO_2 for cryptomelane (-18.6), which has a lower manganese oxidation state, corresponded to the oxygen fugacity in the middle of the yellow laterite and that the log fO_2 values for the top and bottom of the manganese laterite profile (-0.7 and -26.2), respectively, represent the values for the top and bottom of our profile. The remaining log fO_2 values (for pH values of 7 and 7.5) were obtained by interpolation. In Figure 7, we show a representative profile for the giant Goro Ni-Co laterite deposit in New Caledonia, which, in addition to containing large reserves of Ni, also contains 355,000 tons of Co (Slack et al., 2017). Also shown in this figure is the distribution of Co and the corresponding solubility of heterogenite. As can be seen, the concentration of Co is low in the upper part of the profile, increases somewhat with depth and reaches a sharp maximum in the lower part of the yellow laterite, below which it gradually decreases to background values in the saprock. This distribution is roughly duplicated by the solubility of heterogenite, except that the solubility maximum is a little above that of the concentration maximum. To explain these distributions, we propose a model in which, initially, the laterite profile was vanishingly thin, and the solubility maximum was immediately below its upper surface. With progressive weathering, this solubility maximum migrated downwards leaving behind laterite that was strongly depleted in cobalt above a zone in which the greater availability of Co led to its adsorption on lithiophorite and, particularly, cryptomelane. In the upper part of the profile the effect of decreasing fO_2 in promoting solubility (see above) progressively superseded the inhibiting effect of increasing pH with depth, thereby remobilizing the adsorbed cobalt and leading to a solubility maximum at values of fO_2 and pH of ~ -19 log units and 6.5, respectively. Below this maximum, the continued increase in pH eventually outweighed the effect of decreasing fO_2 and led to the saturation of the weathering fluid in heterogenite (and potentially earlier, in absolane) and the development of a cobalt ore body.

Conclusions

Cobalt is a highly compatible metal that reaches its highest concentration in olivine and, thus, in rocks of ultramafic and, to a lesser extent, mafic composition. Economic deposits of Co therefore develop as a result of processes involving ultramafic/mafic magmas and rocks. These processes comprise silicate/sulfide liquid immiscibility, hydrothermal mobilization and weathering. Magmatic Co ores are the products of the separation from ultramafic and mafic magmas of small proportions of sulfide liquids into which the Co partitions strongly and is accompanied by much larger amounts of Ni. Because the Co content of ultramafic (komatiitic) magmas is considerably higher than that of mafic (basaltic) magmas, the Co content of deposits originating from ultramafic magmas is correspondingly higher. Hydrothermal Co deposits fall into two broad classes, sediment-hosted (shales), represented by the Central African Copperbelt, in which Co occurs as sulfides and is subordinate to Cu, and vein-hosted, represented by the Bou Azzer District, Morocco, in which Co occurs as arsenides and sulfarsenides and is the main ore metal. For both classes, the source of the Co was ultramafic rocks, and the ore fluid was a high salinity, oxidized brine derived from the residues of evaporation (sediment-hosted class) or interaction of meteoric or metamorphic fluids with evaporite (vein-hosted class), consistent with the observation that Co forms its most stable complexes with Cl^- and cobalt mineral solubility is favored by high fO_2. Ore deposition, in the case of the sediment-hosted class, occurred in response to the reduction of fO_2 by organic matter in the host shales, and in the vein deposits as a result of pH neutralization by the host diorites and felsic volcanics. The vein-hosted cobalt deposits are dominated by arsenides and form because of the high As to reduced S ratio in the ore fluid. Cobalt deposits resulting from weathering form in laterites developed over olivine-rich ultramafic rocks, e.g., dunites, and their serpentinized equivalents. Weathering fluids that are relatively acidic, as a result of the accumulation of organic matter in a hot, humid tropical environment, leach Co from an olivine-rich precursor and transport it downwards in a developing soil profile where it accumulates in yellow laterite as a result of its adsorption on manganese oxides and subsequent incorporation in absolane (a manganese oxide) and precipitation as heterogenite. In summary, Co deposits ultimately owe their origin to ultramafic and to a lesser extent mafic magmas/rocks and acquire economic concentrations of this metal either through its affinity for sulfur (silicate-sulfide liquid immiscibility) or as a result of its mobilization by aqueous fluids of high or low temperature at favourable conditions of pH, fO_2 and ligand activity (high temperature).

Acknowledgements

The research presented in this paper was funded by a Discovery grant from the National Scientific and Engineering Research Council of Canada (NSERC). Eugeny Bastrakov introduced the authors to the geochemical modelling program Geo TPD, which was used in this paper.

Figure captions

Figure 1 Schematic plan and cross-section showing the development of komatiite-hosted deposits, modified after Barnes et al. (2013).

Figure 2 Cross-sections through komatiite-hosted Kambalda type (a) and Mt Keith type (b) ore deposits, modified after Hoatson et al. (2006).

Figure 3 (a) - A schematic cross-section of a typical Noril'sk-type ore-bearing intrusion (modified after Naldrett, 2004c); 1 - Residual series rocks, 2 - Olivine-bearing gabbrodolerite, 3 - Leucogabbro and upper taxitic gabbrodolerite, 4 - Olivine gabbrodolerite, 5 - Picritic gabbrodolerite, 6 - Lower taxitic gabbrodolerite, 7 - Contact and Lower Olivine gabbrodolerite. 8 - ore. (b) - A schematic cross-section of the Noril'sk intrusions showing the distribution of magmatic sulfide mineralization (inspired by Naldrett, 2004c); 1 - Cambrian-Silurian sedimentary rocks with rare anhydrite layers, 2 - Devonian carbonate-sedimentary rocks with abundant anhydrite layers, 3 - Tungusskaya siliciclastic sedimentary rocks with coal measures, 4 - Siberian flood basalts, 5 - gabbrodolerite intrusions, 6 - ore bodies.

Figure 4 A log fO_2-pH diagram constructed for a fluid containing 15 wt.% NaCl and a 0.003 m S at 150 ºC showing the stability fields of Co minerals in the system Co-O-S and Cu minerals in system Cu-O-S. Also shown are the solubility contours in ppm for Co minerals (blue) and Cu minerals (red) assuming transport of the Co as the species $CoCl_4^{2-}$ and Cu as the species $CuCl^{2-}$. The blue ellipse and red circle represent the initial and final conditions, respectively, for the mineralizing fluid in sedimentary-hosted deposits (the diagram was constructed using the GeoTPD program of Bastrakov and Dick, 2019).

Figure 5 Cartoons of a rift basin illustrating the stages in the formation of sediment-hosted Cu-Co deposits showing (a) the initial state of the basin, (b) the effect of a marine transgression in

forcing fluids into the basement, where they leach metals, and (c) the effect of a marine regression in promoting the flow fluids back into the basin. The model envisages the "pumping" of fluids through seismic activity. 1 - basement, 2 - mafic-ultra-mafic rocks, 3 - evaporitic layers, 4 - organic-rich layers, 5 - other sediments, 6 - sea level, 7 - direction of fluid flow.

Figure 6 (a and b) - A two-stage model for a vein-type Co deposit involving the release of Co from serpentinite to a fluid, its immediate precipitation as Co-sulfides due to reduction of the fluid by serpentinite (a) and its subsequent remobilization in response to a decrease in the fO_2 buffering capacity of the serpentinite (b). (c and d) - Schematic log fO_2-pH diagrams showing the evolution of the Co-As-S paragenesis from skutterudite to an alternation of safflorite and cobaltite in response to an increase in fO_2 and a decrease in pH (c) or a decrease in the As:S (reduced) ratio (d).

Figure 7 A schematic laterite profile showing the distribution of Co concentrations for the various zones in the giant Goro Ni-Co laterite deposit, New Caledonia, and the changing of the solubility of heterogenite with depth in response to oxygen fugacity and pH (the profile was modified from Elias, 2002, and the Co concentrations were taken from Wells et al., 2009). See the main text for an explanation of how the solubility profile was constructed.

References

Abzalov, M. Z., and Both, R. A., 1997, The Pechenga Ni-Cu deposits, Russia: Data on PGE and Au distribution and sulphur isotope compositions: Mineralogy and Petrology, v. 61, p. 119-143.

Álvaro, J. J., Ezzouhairi, H., Vennin, E., Ribeiro, M. L., Clausen, S., Charif, A., Ayad, N. A., and Moreira, M. E., 2006, The Early-Cambrian Boho volcano of the El Graara massif, Morocco: Petrology, geodynamic setting and coeval sedimentation: Journal of African Earth Sciences, v. 44, p. 396-410.

Álvaro, J. J., Macouin, M., Ezzouhairi, H., Charif, A., Ayad, N. A., Ribeiro, M. L., and Ader, M., 2008, Late Neoproterozoic carbonate productivity in a rifting context: the Adoudou Formation and its associated bimodal volcanism onlapping the western Saghro inlier, Morocco: Geological Society, London, Special Publications, v. 297, p. 285.

Annels, A. E., and Simmonds, J. R., 1984, Cobalt in the Zambian Copperbelt: Precambrian Research, v. 25, p. 75-98.

Arndt, N. T., Czamanske, G. K., Walker, R. J., Chauvel, C., and Fedorenko, V. A., 2003, Geochemistry and Origin of the Intrusive Hosts of the Noril'sk-Talnakh Cu-Ni-PGE Sulfide Deposits: Economic Geology, v. 98, p. 495-515.

Barnes, S.-J., and Naldrett, A. J., 1986, Variations in platinum group element concentrations in the Alexo mine komatiite, Abitibi greenstone belt, northern Ontario: Geological Magazine, v. 123, p. 515-524.

Barnes, S. J., Heggie, G. J., and Fiorentini, M. L., 2013, Spatial Variation in Platinum Group Element Concentrations in Ore-Bearing Komatiite at the Long-Victor Deposit, Kambalda Dome, Western Australia: Enlarging the Footprint of Nickel Sulfide Orebodies: Economic Geology, v. 108, p. 913-933.

Bastrakov, E. N., and Dick, J., 2019, GeoTPD — an interactive online tool for geochemical modelling for the broad geological community Goldschmidt Conference.

Beaudoin, G., and Therrien, P., 2009, The web stable isotope fractionation calculator, *in* De Groot, P. A., ed., Handbook of stable isotopes analytical techniques, 2, Elsevier, p. 1054–1047.

Bouabdellah, M., Maacha, L., Levresse, G., and Saddiqi, O., 2016, The Bou Azzer Co–Ni–Fe–As(±Au ± Ag) District of Central Anti-Atlas (Morocco): A Long-Lived Late Hercynian to Triassic Magmatic-Hydrothermal to Low-Sulphidation Epithermal System, *in* Bouabdellah, M., and Slack, J. F., eds., Mineral Deposits of North Africa: Cham, Springer International Publishing, p. 229-247.

Brand, N. W., Butt, C. R. M., and Elías, M., 1998, Nickel laterites: classification and features: AGSO Journal of Australian Geology & Geophysics, 1998, p. 81-88.

Bull, S., Selley, D., Broughton, D., Hitzman, M., Cailteux, J., Large, R., and McGoldrick, P., 2011, Sequence and carbon isotopic stratigraphy of the Neoproterozoic Roan Group strata of the Zambian copperbelt: Precambrian Research, v. 190, p. 70-89.

Butt, C. R. M., and Cluzel, D., 2013, Nickel laterite ore deposits: Weathered serpentinites: Elements, v. 9, p. 123-128.

Cailteux, J. L. H., Kampunzu, A. B., Lerouge, C., Kaputo, A. K., and Milesi, J. P., 2005, Genesis of sediment-hosted stratiform copper–cobalt deposits, central African Copperbelt: Journal of African Earth Sciences, v. 42, p. 134-158.

Campbell, I. H., Czamanske, G. K., Fedorenko, V. A., Hill, R. I., and Stepanov, V., 1992, Synchronism of the Siberian Traps and the Permian-Triassic Boundary: Science, v. 258, p. 1760-1763.

Davey, J. E., 2019, Anomalous metal enrichment of Basin Brines in the Zambian Copperbelt: a comparison of fluid chemistry in contrasting sediment-hosted copper systems, University of Southampton, 250 p.

Dewaele, S., Muchez, P., Vets, J., Fernandez-Alonzo, M., and Tack, L., 2006, Multiphase origin of the Cu–Co ore deposits in the western part of the Lufilian fold-and-thrust belt, Katanga (Democratic Republic of Congo): Journal of African Earth Sciences, v. 46, p. 455-469.

Di Benedetto, F., Costagliola, P., Benvenuti, M., Lattanzi, P., Romanelli, M., and Tanelli, G., 2006, Arsenic incorporation in natural calcite lattice: Evidence from electron spin echo spectroscopy: Earth and Planetary Science Letters, v. 246, p. 458-465.

Dolansky, L. M., 2007, Controls on the genesis of hydrothermal cobalt mineralization: insights from the mineralogy and geochemistry of the Bou Azzer deposits, Morocco, McGill University Libraries, 192 p.

Duchesne, J.-C., Liégeois, J.-P., Deblond, A., and Tack, L., 2004, Petrogenesis of the Kabanga–Musongati layered mafic–ultramafic intrusions in Burundi (Kibaran Belt): geochemical, Sr–Nd isotopic constraints and Cr–Ni behaviour: Journal of African Earth Sciences, v. 39, p. 133-145.

El Desouky, H. A., Muchez, P., Boyce, A. J., Schneider, J., Cailteux, J. L. H., Dewaele, S., and von Quadt, A., 2010, Genesis of sediment-hosted stratiform copper–cobalt mineralization at Luiswishi and Kamoto, Katanga Copperbelt (Democratic Republic of Congo): Mineralium Deposita, v. 45, p. 735-763.

El Desouky, H. A., Muchez, P., and Cailteux, J., 2009, Two Cu–Co sulfide phases and contrasting fluid systems in the Katanga Copperbelt, Democratic Republic of Congo: Ore Geology Reviews, v. 36, p. 315-332.

El Hadi, H., Simancas, J. F., Martínez-Poyatos, D., Azor, A., Tahiri, A., Montero, P., Fanning, C. M., Bea, F., and González-Lodeiro, F., 2010, Structural and geochronological constraints on the evolution of the Bou Azzer Neoproterozoic ophiolite (Anti-Atlas, Morocco): Precambrian Research, v. 182, p. 1-14.

Elias, M., 2002, Nickel laterite deposits-geological overview, resources and exploitation, Centre for Ore Deposit Research, 4: University of Tasmania, Special Publication, p. 205-220.

En-Naciri, A., Barbanson, L., and Touray, J.-C., 1997, Brine inclusions from the Co-As(Au) Bou Azzer District, Anti-Atlas Mountains, Morocco: Economic Geology, v. 92, p. 360-367.

Erdoğan, Y., Aksu, M., Demirbaş, A., and Abalı, Y., 1998, Analyses of boronic ores and sludges and solubilities of boron minerals in CO2-saturated water: Resources, Conservation and Recycling, v. 24, p. 275-283.

Freyssinet, P., Butt, C. R. M., Morris, R. C., and Piantone, P., 2005, Ore-forming processes related to lateritic weathering, *in* Hedenquist, J. W., Thomson, J. F. H., Goldfarb, R. J., and Richards, J. P., eds., Economic Geology 100th Anniversary Volume, Economic Geology Publishing Company, New Haven, Connecticut, p. 681-722.

Gasquet, D., Levresse, G., Cheilletz, A., Azizi-Samir, M. R., and Mouttaqi, A., 2005, Contribution to a geodynamic reconstruction of the Anti-Atlas (Morocco) during Pan-African times with

the emphasis on inversion tectonics and metallogenic activity at the Precambrian–Cambrian transition: Precambrian Research, v. 140, p. 157-182.

Gleeson, S. A., Herrington, R. J., Durango, J., Velásquez, C. A., and Koll, G., 2004, The Mineralogy and Geochemistry of the Cerro Matoso S.A. Ni Laterite Deposit, Montelíbano, Colombia: Economic Geology, v. 99, p. 1197-1213.

Golightly, J. P., 1981, Nickeliferous laterite deposits: Economic Geology 75th anniversary volume, p. 710-735.

Gorbachev, N. S., and Grinenko, L. N., 1973, The sulfur-isotope ratios of the sulfides and sulfates of the Oktyabr'sky sulfide deposit, Norilsk region, and the problem of its origin: Geokhimiya, v. 8, p. 1127–1136.

Greyling, L. N., 2009, Fluid evolution and characterisation of mineralising solutions in the Central African Copperbelt, University of the Witwatersrand.

Guillemette, N., and Williams-Jones, A. E., 1993, Genesis of the Sb-W-Au deposits at Ixtahuacan, Guatemala: evidence from fluid inclusions and stable isotopes: Mineralium Deposita : International Journal of Geology, Mineralogy and Geochemistry of Mineral Deposits, v. 28, p. 167-180.

Halls, C., and Stumpfl, E., 1972, The five-element (Ag-Bi-Co-Ni-As) vein deposit – A critical appraisal of the geological environments in which it occurs and of the theories affecting its origin: 24th International Geological Congress, Montreal, 1972.

Hanski, E. J., Luo, Z.-Y., Oduro, H., Walker, R. J., Li, C., and Ripley, E. M., 2011, The Pechenga Ni-Cu Sulfide Deposits, Northwestern Russia: A Review with New Constraints from the Feeder Dikes, Magmatic Ni-Cu and PGE Deposits: Geology, Geochemistry, and Genesis, 17, Society of Economic Geologists, p. 0.

Hanski, E. J., and Smolkin, V. F., 1995, Iron- and LREE-enriched mantle source for early Proterozoic intraplate magmatism as exemplified by the Pechenga ferropicrites, Kola Peninsula, Russia: Lithos, v. 34, p. 107-125.

Haynes, D. W., 1986, Stratiform copper deposits hosted by low-energy sediments; II, Nature of source rocks and composition of metal-transporting water: Economic Geology, v. 81, p. 266-280.

Helvaci, C., and Alonso, R. N., 2000, Borate Deposits of Turkey and Argentina; A Summary and Geological Comparison: Turkish Journal of Earth Sciences, v. 9, p. 1-27.

Hitzman, M., Kirkham, R., Broughton, D., Thorson, J., Selley, D., Hedenquist, J. W., Thompson, J. F. H., Goldfarb, R. J., and Richards, J. P., 2005, The sediment-hosted stratiform copper ore system, One Hundredth Anniversary Volume, Society of Economic Geologists, p. 0.

Hoatson, D. M., Jaireth, S., and Jaques, A. L., 2006, Nickel sulfide deposits in Australia: Characteristics, resources, and potential: Ore Geology Reviews, v. 29, p. 177-241.

Hoepffner, C., Soulaimani, A., and Piqué, A., 2005, The Moroccan Hercynides: Journal of African Earth Sciences, v. 43, p. 144-165.

Houlé, M. G., Lesher, C. M., and Davis, P. C., 2012, Thermomechanical erosion at the Alexo Mine, Abitibi greenstone belt, Ontario: implications for the genesis of komatiite-associated Ni-Cu-(PGE) mineralization: Mineralium Deposita, v. 47, p. 105-128.

Huppert, H. E., Sparks, R. S. J., Turner, J. S., and Arndt, N. T., 1984, Emplacement and cooling of komatiite lavas: Nature, v. 309, p. 19-22.

Iacono-Marziano, G., Ferraina, C., Gaillard, F., Di Carlo, I., and Arndt, N. T., 2017, Assimilation of sulfate and carbonaceous rocks: Experimental study, thermodynamic modeling and application to the Noril'sk-Talnakh region (Russia): Ore Geology Reviews, v. 90, p. 399-413.

Jugo, P. J., 2009, Sulfur content at sulfide saturation in oxidized magmas: Geology, v. 37, p. 415-418.

Kampschulte, A., and Strauss, H., 2004, The sulfur isotopic evolution of Phanerozoic seawater based on the analysis of structurally substituted sulfate in carbonates: Chemical Geology, v. 204, p. 255-286.

Key, R. M., Liyungu, A. K., Njamu, F. M., Somwe, V., Banda, J., Mosley, P. N., and Armstrong, R. A., 2001, The western arm of the Lufilian Arc in NW Zambia and its potential for copper mineralization: Journal of African Earth Sciences, v. 33, p. 503-528.

Krivolutskaya, N. A., Kuzmin, D. V., Gongalsky, B. I., Roshchina, I. A., Kononkova, N. N., Svirskaya, N. M., and Romashova, T. V., 2018, Stages of Trap Magmatism in the Norilsk Area: New Data on the Structure and Geochemistry of the Volcanic Rocks: Geochemistry International, v. 56, p. 419-437.

Lafay, R., Montes-Hernandez, G., Janots, E., Munoz, M., Auzende, A. L., Gehin, A., Chiriac, R., and Proux, O., 2016, Experimental investigation of As, Sb and Cs behavior during olivine serpentinization in hydrothermal alkaline systems: Geochimica et Cosmochimica Acta, v. 179, p. 177-202.

Leblanc, M., and Billaud, P., 1982, Cobalt arsenide orebodies related to an upper Proterozoic ophiolite; Bou Azzer (Morocco): Economic Geology, v. 77, p. 162-175.

Lesher, C. M., and Groves, D. I., 1986, Controls on the Formation of Komatiite-Associated Nickel-Copper Sulfide Deposits: Geology and Metallogeny of Copper Deposits, Berlin, Heidelberg, 1986//, 1986, p. 43-62.

Levresse, G., 2001, Contribution à l'établissement d'un modèle génétique des gisements d'Imiter (Ag-Hg), Bou Madine (Pb-Zn-Cu-Ag-Au) et Bou Azzer (Co-Ni-As-Au-Ag) dans l'Anti-Atlas marocain, Institut National Polytechnique de Lorraine.

Li, C., and Naldrett, A. J., 1999, Geology and petrology of the Voisey's Bay intrusion: reaction of olivine with sulfide and silicate liquids: Lithos, v. 47, p. 1-31.

Lightfoot, P. C., Hawkesworth, C. J., Hergt, J., Naldrett, A. J., Gorbachev, N. S., Fedorenko, V. A., and Doherty, W., 1993, Remobilisation of the continental lithosphere by a mantle plume: major-, trace-element, and Sr-, Nd-, and Pb-isotope evidence from picritic and tholeiitic lavas of the Noril'sk District, Siberian Trap, Russia: Contributions to Mineralogy and Petrology, v. 114, p. 171-188.

Lin, J., Chen, N., Nilges, M. J., and Pan, Y., 2013, Arsenic speciation in synthetic gypsum (CaSO4·2H2O): A synchrotron XAS, single-crystal EPR, and pulsed ENDOR study: Geochimica et Cosmochimica Acta, v. 106, p. 524-540.

Llorca, S. M., 1993, Metallogeny of supergene cobalt mineralization, New Caledonia: Australian Journal of Earth Sciences, v. 40, p. 377-385.

Maacha, L., Azizi, R., and Bouchta, R., , 1998, Gisements cobaltifères du district de Bou Azzer (Anti-Atlas): structure, minéralogie et conditions de genèse: Chronique de la Recherche Minière, v. 531-532, p. 65-75.

Malitch, K. N., Latypov, R. M., Badanina, I. Y., and Sluzhenikin, S. F., 2014, Insights into ore genesis of Ni-Cu-PGE sulfide deposits of the Noril'sk Province (Russia): Evidence from copper and sulfur isotopes: Lithos, v. 204, p. 172-187.

Maloof, A. C., Schrag, D. P., Crowley, J. L., and Bowring, S. A., 2005, An expanded record of Early Cambrian carbon cycling from the Anti-Atlas Margin, Morocco: Canadian Journal of Earth Sciences, v. 42, p. 2195-2216.

Master, S., Rainaud, C., Armstrong, R. A., Phillips, D., and Robb, L. J., 2005, Provenance ages of the Neoproterozoic Katanga Supergroup (Central African Copperbelt), with implications for basin evolution: Journal of African Earth Sciences, v. 42, p. 41-60.

Mavrogenes, J. A., and O'Neill, H. S. C., 1999, The relative effects of pressure, temperature and oxygen fugacity on the solubility of sulfide in mafic magmas: Geochimica et Cosmochimica Acta, v. 63, p. 1173-1180.

Melezhik, V. A., Grinenko, L. N., and Fallick, A. E., 1998, 2000-Ma sulphide concretions from the `Productive' Formation of the Pechenga Greenstone Belt, NW Russia: genetic history based on morphological and isotopic evidence: Chemical Geology, v. 148, p. 61-94.

Melezhik, V. A., Hudson-Edwards, K. A., Green, A. N., and Grinenko, L. N., 1994, Pechenga area Russia - Part 2: nickel-copper deposits and related rocks: Trans Instn Mining Metall (Section B: Applied Earth Sei), v. 103, p. B87-162.

Melezhik, V. A., and Sturt, B. A., 1994, General geology and evolutionary history of the early proterozoic Polmak-Pasvik-Pechenga-Imandra/Varzuga-Ust'Ponoy greenstone belt in the northeastern Baltic Shield: Earth-Science Reviews, v. 36, p. 205-241.

Mifdal, A., and Peucat, J.-J., 1985, Datations U-Pb et Rb-Sr du volcanisme acide de l'Anti-Atlas Marocain et du socle sous-jacent dans la région de Ouarzazate apport au problème de la limite Précambrien-Cambrien: Sciences Géologiques, Bulletin, v. 38, p. 185-200.

Naldrett, A. J., 2004a, Deposits of the Pechenga area, Russia, *in* Naldrett, A. J., ed., Magmatic Sulfide Deposits: Geology, Geochemistry and Exploration: Berlin, Heidelberg, Springer Berlin Heidelberg, p. 279-306.

Naldrett, A. J., 2004b, Komatiite-Related Deposits, *in* Naldrett, A. J., ed., Magmatic Sulfide Deposits: Geology, Geochemistry and Exploration: Berlin, Heidelberg, Springer Berlin Heidelberg, p. 67-136.

Naldrett, A. J., 2004c, Ore deposits associated with flood basalt volcanism, Magmatic Sulfide Deposits: Geology, Geochemistry and Exploration: Berlin, Heidelberg, Springer Berlin Heidelberg, p. 137-278.

Naldrett, A. J., 2004d, Voisey's Bay and other deposits, Labrador, Canada, *in* Naldrett, A. J., ed., Magmatic Sulfide Deposits: Geology, Geochemistry and Exploration: Berlin, Heidelberg, Springer Berlin Heidelberg, p. 307-372.

Naldrett, A. J., Fedorenko, V. A., Asif, M., Lin, S., Kunilov, V. E., Stekhin, A. I., Lightfoot, P. C., and Gorbachev, N. S., 1996, Controls on the composition of Ni-Cu sulfide deposits as illustrated by those at Noril'sk, Siberia: Economic Geology, v. 91, p. 751-773.

Naldrett, A. J., Hoffman, E. L., Green, A. H., Chou, C. L., Naldrett, S. R., and Alcock, R. A., 1979, The composition of Ni-sulfide ores, with particular reference to their content of PGE and Au: Canadian Mineralogist, v. 17, p. 403-415.

Oberthür, T., Melcher, F., Henjes-Kunst, F., Gerdes, A., Stein, H., Zimmerman, A., and El Ghorfi, M., 2009, Hercynian age of the cobalt-nickel-arsenide-(gold) ores, Bou Azzer, Anti-Atlas, Morocco: Re-Os, Sm-Nd, and U-Pb age determinations: Economic Geology, v. 104, p. 1065-1079.

Ohmoto, H., 1986, Stable isotope geochemistry of ore deposits, *in* Valley, J. W., Taylor, H. P., and O'Neil, J. R., eds., Stable isotopes in high temperature geological processes, 16. Reviews in Mineralogy and Geochemistry: Washington, D.C., Mineralogical Society of America, p. 491-556.

Parc, S., Nahon, D., Tardy, Y., and Vieillard, P., 1989, Estimated solubility products and fields of stability for cryptomelane, nsutite, birnessite, and lithiophorite based on natural lateritic weathering sequences: American Mineralogist, v. 74, p. 466-475.

Porada, H., and Berhorst, V., 2000, Towards a new understanding of the Neoproterozoic-early palæozoic Lufilian and northern Zambezi belts in Zambia and the Democratic Republic of Congo: Journal of African Earth Sciences, v. 30, p. 727-771.

Ripley, E. M., Park, Y.-R., Li, C., and Naldrett, A. J., 1999, Sulfur and oxygen isotopic evidence of country rock contamination in the Voisey's Bay Ni–Cu–Co deposit, Labrador, Canada: Lithos, v. 47, p. 53-68.

Scharrer, M., Kreissl, S., and Markl, G., 2019, The mineralogical variability of hydrothermal native element-arsenide (five-element) associations and the role of physicochemical and kinetic factors concerning sulfur and arsenic: Ore Geology Reviews, v. 113, p. 103025.

Selley, D., Scott, R., Emsbo, P., Koziy, L., Hitzman, M. W., Bull, S. W., Duffett, M., Sebagenzi, S., Halpin, J., and Broughton, D. W., 2018, Structural Configuration of the Central African Copperbelt: Roles of Evaporites in Structural Evolution, Basin Hydrology, and Ore Location, *in* Arribas R, A. M., and Mauk, J. L., eds., Metals, Minerals, and Society, 21, Society of Economic Geologists (SEG), p. 0.

Shvarov, Y. V., and Bastrakov, E. N., 1999, HCh: a software package for geochemical equilibrium modelling. User's Guide.: Record 1999/25, Australian Geological Survey Organisation, 61 p.

Slack, J. F., Kimball, B. E., and Shedd, K. B., 2017, Critical mineral resources of the United States—Economic and environmental geology and prospects for future supply, *in* Schulz, K. J., DeYoung, J. J. H., Seal Ii, R. R., and Bradley, D. C., eds., Professional Paper: Reston, VA, p. 862.

Taylor, C. D., Causey, J. D., Denning, P. D., Hammarstrom, J. M., Hayes, T. S., Horton, J. D., Kirschbaum, M. J., Parks, H. L., Wilson, A. B., Wintzer, N. E., and Zientek, M. L., 2013, Descriptive Models, Grade-Tonnage Relations, and Databases for the Assessment of Sediment-Hosted Copper Deposits—With Emphasis on Deposits in the Central African Copperbelt, Democratic Republic of the Congo and Zambia, p. U.S. Geological Survey Scientific Investigations Report 2010–5090–J, 154 p. and data files.

van der Ent, A., Baker, A. J. M., van Balgooy, M. M. J., and Tjoa, A., 2013, Ultramafic nickel laterites in Indonesia (Sulawesi, Halmahera): Mining, nickel hyperaccumulators and opportunities for phytomining: Journal of Geochemical Exploration, v. 128, p. 72-79.

Wells, M. A., Ramanaidou, E. R., Verrall, M., and Tessarolo, C., 2009, Mineralogy and crystal chemistry of "garnierites" in the Goro lateritic nickel deposit, New Caledonia: European Journal of Mineralogy, v. 21, p. 467-483.

Williams-Jones, A. E., and Vasyukova, O. V., 2018, The economic geology of scandium, the runt of the rare earth element litter: Economic Geology, v. 113, p. 973-988.

Williams-Jones, A. E., and Vasyukova, O. V., 2021, Constraints on the Genesis of Cobalt Deposits: Part I, Theoretical Considerations: Economic Geology

Williams, D. A., Kerr, R. C., and Lesher, C. M., 2011, Mathematical modeling of thermomechanical erosion beneath Proterozoic komatiitic basaltic sinuous rilles in the Cape Smith Belt, New Qu,bec, Canada: Mineralium Deposita, v. 46, p. 943-958.

1113

Table 1. The formulae of cobalt minerals referred to in this paper

Asbolane	$(Ni,Co)_{2-x}Mn^{4+}(O,OH)_4 \cdot nH_2O)$
Carrollite	$Cu(Co,Ni)_2S_4$
Cattierite	CoS_2
Cobaltite	$CoAsS$
Cobaltpentlandite	$(Co,Ni,Fe)_9S_8$
Heterogenite	$CoO(OH)$
Linnaeite	$Co^{2+}Co^{3+}{}_2S_4$
Safflorite	$(Co,Ni,Fe)As_2$
Siegenite	$CoNi_2S_4$
Skutterudite	$CoAs_3$

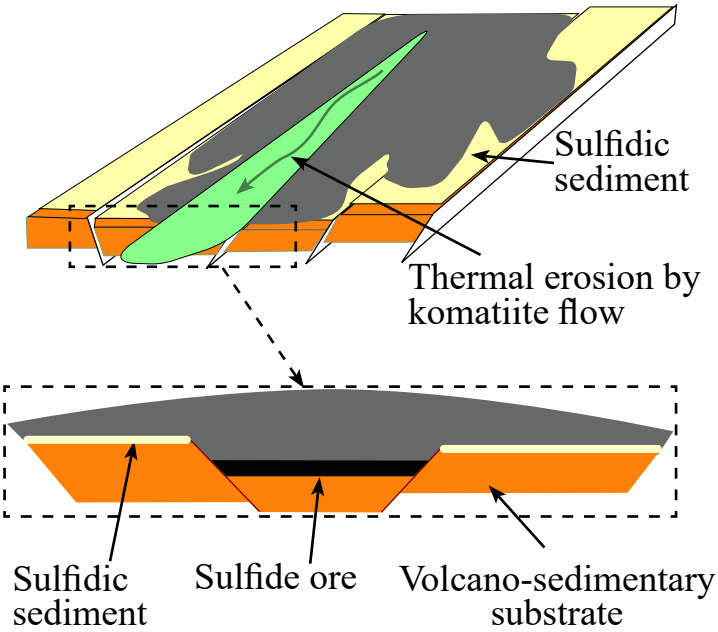

Figure 1 Schematic plan and cross-section showing the development of komatiite-hosted deposits, modified after Barnes et al. (2013)

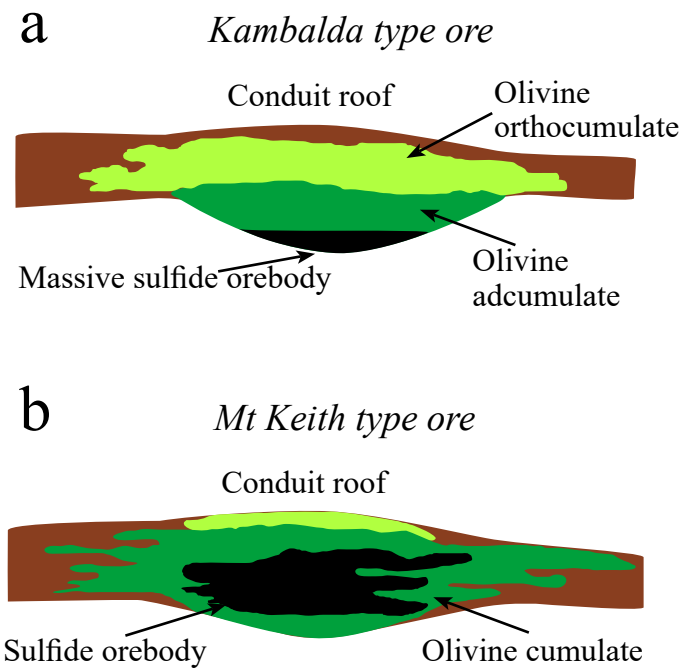

Figure 2 Cross-sections through komatiite-hosted Kambalda type (a) and Mt Keith type (b) ore deposits, modified after Hoatson et al. (2006).

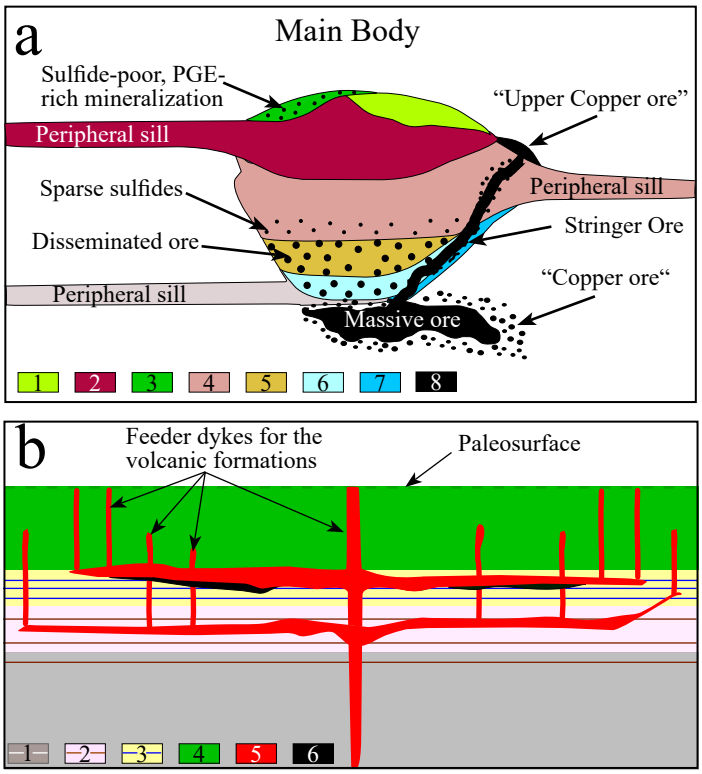

Figure 3 (a) - A schematic cross-section of a typical Noril'sk-type ore-bearing intrusion (modified after Naldrett, 2004c); 1 - Residual series rocks, 2 - Olivine-bearing gabbrodolerite, 3 - Leucogabbro and upper taxitic gabbrodolerite, 4 - Olivine gabbrodolerite, 5 - Picritic gabbrodolerite, 6 - Lower taxitic gabbrodolerite, 7 - Contact and Lower Olivine gabbrodolerite. 8 - ore. (b) - A schematic cross-section of the Noril'sk intrusions showing the distribution of magmatic sulfide mineralization (inspired by Naldrett, 2004c); 1 - Cambrian-Silurian sedimentary rocks with rare anhydrite layers, 2 - Devonian carbonate-sedimentary rocks with abundant anhydrite layers, 3 - Tungusskaya siliciclastic sedimentary rocks with coal measures, 4 - Siberian flood basalts, 5 - gabbrodolerite intrusions, 6 - ore bodies.

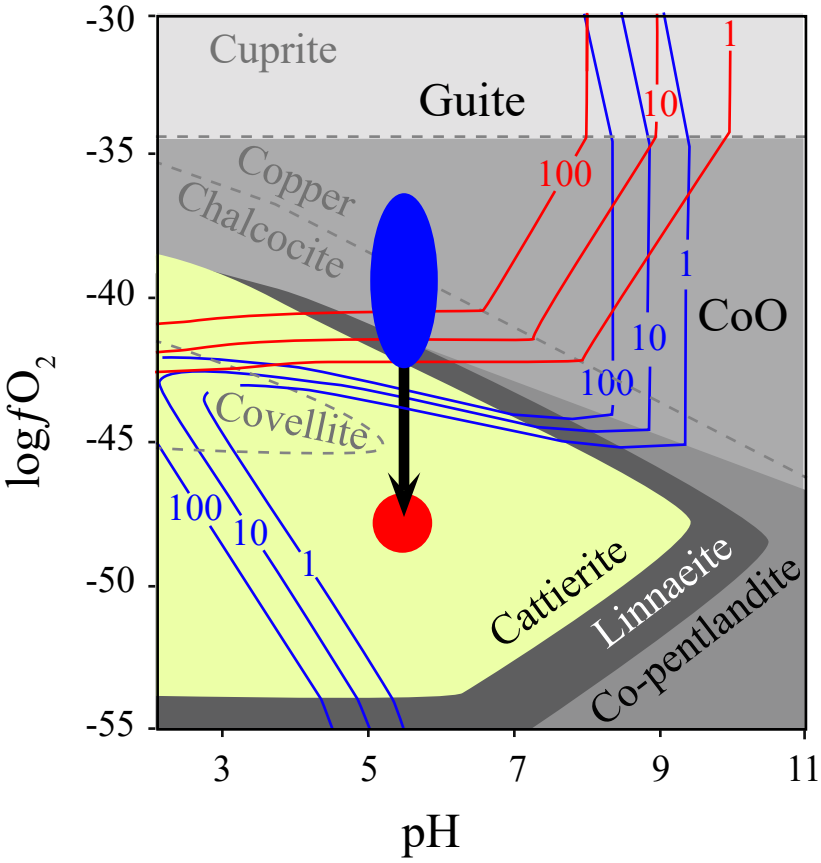

Figure 4 A log fO_2-pH diagram constructed for a fluid containing 15 wt.% NaCl and a 0.003 m S at 150 °C showing the stability fields of Co minerals in the system Co-O-S and Cu minerals in system Cu-O-S. Also shown are the solubility contours in ppm for Co minerals (blue) and Cu minerals (red) assuming transport of the Co as the species $CoCl_4^{2-}$ and Cu as the species $CuCl^{2-}$. The blue ellipse and red circle represent the initial and final conditions, respectively, for the mineralizing fluid in sedimentary-hosted deposits (the diagram was constructed using the GeoTPD program of Bastrakov and Dick, 2019).

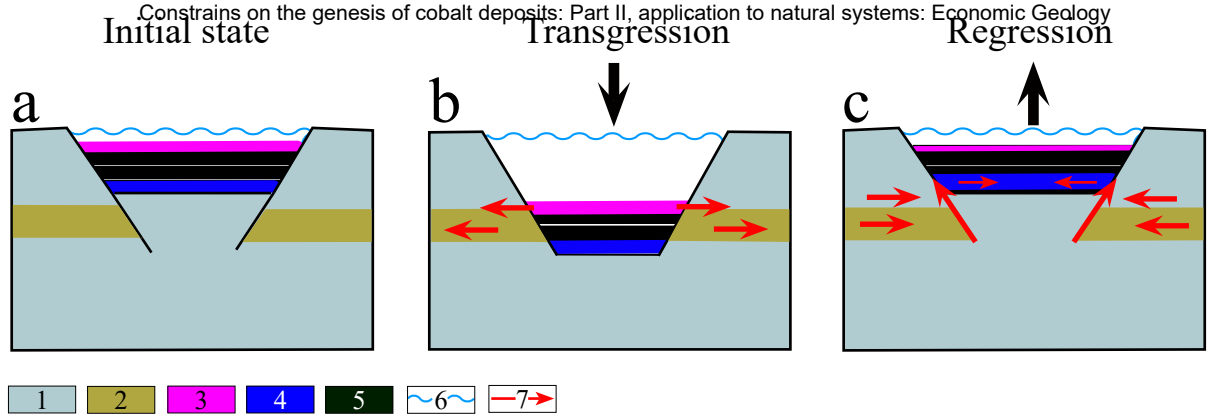

Figure 5 Cartoons of a rift basin illustrating the stages in the formation of sediment-hosted Cu-Co deposits showing (a) the initial state of the basin, (b) the effect of a marine transgression in forcing fluids into the basement, where they leach metals, and (c) the effect of a marine regression in promoting the flow fluids back into the basin. The model envisages the "pumping" of fluids through seismic activity. 1 - basement, 2 - mafic-ultra-mafic rocks, 3 - evaporitic layers, 4 - organic-rich layers, 5 - other sediments, 6 - sea level, 7 - direction of fluid flow.

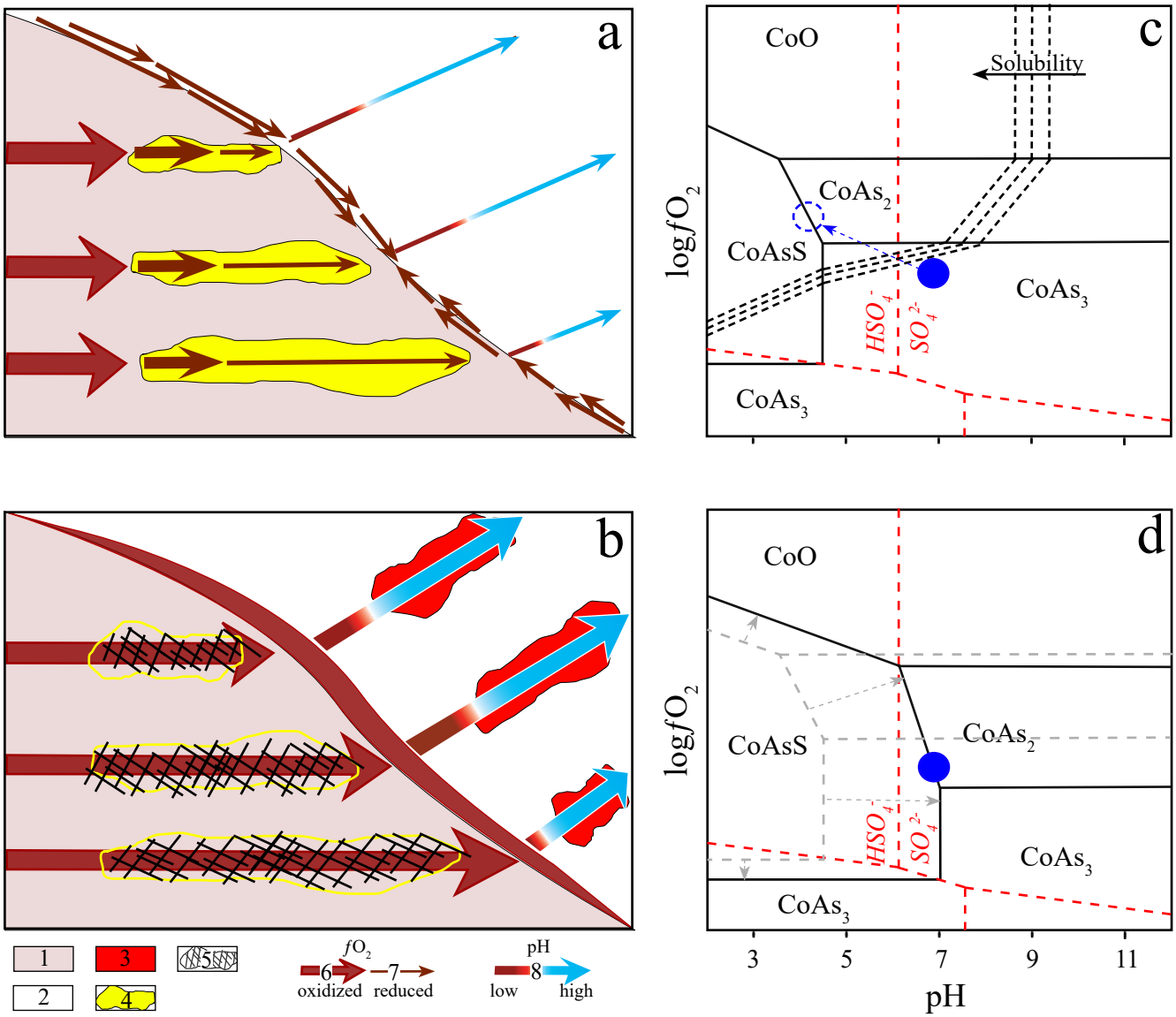

Figure 6 (a and b) - A two-stage model for a vein-type Co deposit involving the release of Co from serpentinite to a fluid, its immediate precipitation as Co-sulfides due to reduction of the fluid by serpentinite (a) and its subsequent remobilization in response to a decrease in the fO_2 buffering capacity of the serpentinite (b). (c and d) - Schematic log fO2-pH diagrams showing the evolution of the Co-As-S paragenesis from skutterudite to an alternation of safflorite and cobaltite in response to an increase in fO_2 and a decrease in pH (c) or a decrease in the As:S (reduced) ratio (d).

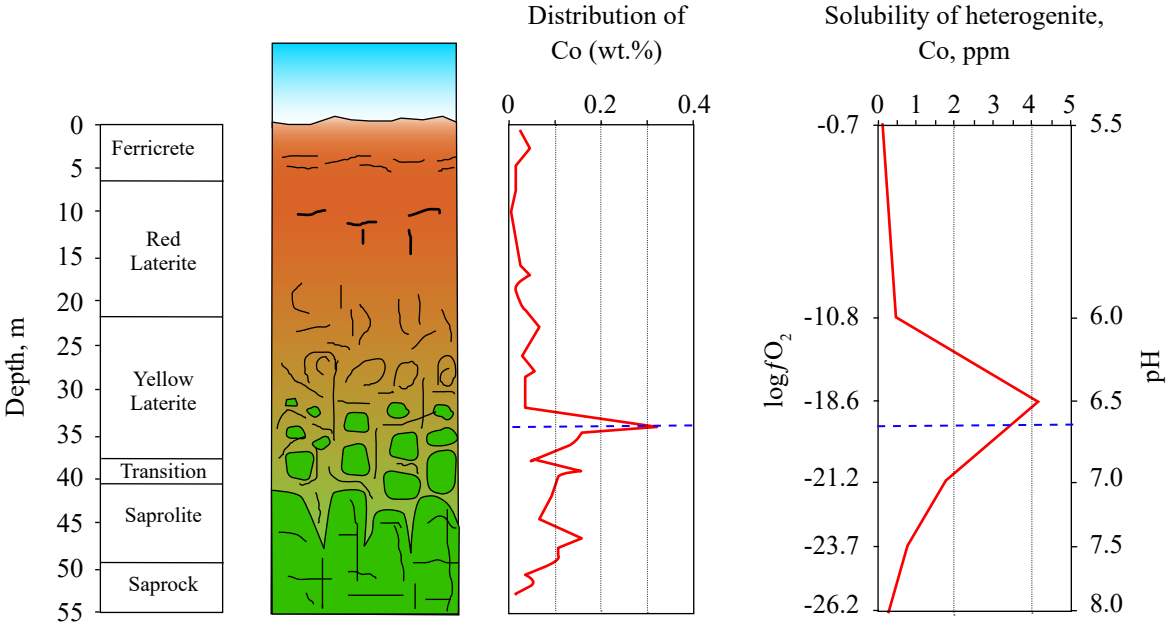

Figure 7 A schematic laterite profile showing the disribution of Co concentrations for the various zones in the giant Goro Ni-Co laterite deposit, New Caledonia, and the changing of the solubility of heterogenite with depth in response to oxygen fugacity and pH (the profile was modified from Elias, 2002, and the Co concentrations were taken from Wells et al., 2009). See the main text for an explanation of how the solubility profile was constructed.